Demographics and Posterior Knee Capsule Histologic and Genetic Characterization in Patients with Severe Knee Osteoarthritis: Comparing Those With Contracture to Those Without Contracture

Thesis submitted to the Department of Biochemistry, Microbiology, and Immunology in partial fulfillment of the requirements for the degree of Masters in Science: Biochemistry

August 2012,
University Of Ottawa

Thomas Mark Campbell

Acknowledgements

Thesis Supervisors:
Dr. Guy Trudel
Dr. Odette Laneuville

Thesis Advisory Committee Members:
Dr. Alain Stintzi
Dr. Zhara Montazeri
Dr. Julian Little

Contributing Partners
Dr. Hans Uhthoff
Mrs. Louise Pelletier and the University of Ottawa Pathology Department
Mrs. Elizabeth Coletta
Mrs. Ying Nie Ping
Dr. Mathew Quon
Dr. Natalie Buminov
Génome Québec

Orthopedic Research Department:
Mrs. Sarah Plamondon
Mrs. Anna Fazekas

Orthopedic Surgeons
Dr. Dervin
Dr. Kim
Dr. Feibel
Dr. Thurston
Dr. Beaulé

Moral Support
Mrs. Claire de Lucovich

Financial Support:
Funding for this project provided by a grant from the Canadian Institutes of Health Research awarded to Dr. Laneuville and Dr. Trudel

Table of Contents

List of Abbreviations

Abbreviation	Term
BMI	Body mass index
cDNA	Complementary deoxyribonucleic acid
CHAD	Chondroadherin
CILP	Cartilage intermediate layer protein, nucleotide pyrophosphohydrolase
COX	Cyclooxygenase
cRNA	Complementary ribonucleic acid
CSN1S1	Casein alpha s1
Cyr61	Cysteine-rich angiogenic inducer
DAB	Diaminobenzidine
ddPCR	Differential display polymerase chain reaction
DNA	Deoxyribonucleic acid
EB	Empirical base
ECM	Extracellular matrix
GS	Gel stain
HIER	Heat-induced epitode retrieval
HMG	High mobility-group box
HPF	High powered field
IHC	Immunohistochemistry
Max	Maximum
MF	Myofibroblasts
Min	Minimum
MMP	Matrix metalloproteinase
OA	Osteoarthritis
OR	Operating room
PCA	Principle component analysis
PCR	Polymerase chain reaction
PROM	Passive range of motion
QN	Quantile normalization
RA	Rheumatoid arthritis
rAAV	Recombinant adeno-associated virus
RGB	Red green blue
RIN	Ribonucleic acid index number
RMA	Robust multiarray average
RNA	Ribonucleic acid
ROM	Range of motion
RPM	Revolutions per minute
RQI	Ribonucleic acid quality index
RT-PCR	Reverse transcriptase polymerase chain reaction
Sox9	Sex determining region Y box-9
TBS	Tris-buffered saline
TGF-β1	Transforming growth factor beta 1
TIMP	Tissue inhibitors of matrix metalloproteinases
TKA	Total knee arthroplasty
VST	Variance stabilization transformation
W&S	Wright and Simon
α-SMA	α smooth muscle actin

List of Figures

List of Tables

Abstract

Introduction: Knee flexion contractures have a negative impact on function for patients with osteoarthritis (OA). Those with contracture treated with total knee arthroplasty (TKA) have more post-operative pain and worse outcome. Little knowledge is available about patient demographic factors or gene expression in the knee joint capsule in the setting of contracture and severe OA.

Methods: Subjects with primary severe knee OA awaiting a TKA were recruited. We collected subject demographic factors that may be associated with preoperative knee contracture. Subjects' posterior knee capsule was harvested intraoperatively. Capsule histological analysis was performed using light microscopy. Gene expression analysis was performed using whole genome microarray and immunohistochemistry was used for protein production analysis comparing those with contracture to those without.

Results: Twenty subjects were recruited for the demographics portion of the study (13 contractures and 7 controls), and capsules from 12 subjects (6 contractures, 6 controls) were used for histology, microarray, and IHC analyses. Contracture subjects had longer duration of OA, reduced extension in the contralateral knee, and showed a trend toward elevated body mass index. Tissue cross-sectional areas of adipose, non-adipose and synovial tissues were not statistically different histologically between the two groups. There was increased expression in the contracture group for the genes CHAD, Cyr61, and Sox9. There was a corresponding increase in protein production for CHAD and Sox9.

Conclusions: Screening for OA duration and bilateral knee range of motion (ROM) could be functionally beneficial. When a knee joint contracture is present, correcting for the resulting leg length discrepancy pre- and post-operatively could improve patient outcome. Gene protein products linking capsular cells to the ECM can influence capsular fibrosis and potentially impact ROM.

Introduction

A joint contracture is a limitation in the passive range of motion (PROM) of a joint [1]. Changes in articular structures (bone, cartilage, capsule) and non-articular structures (ligament, muscle, tendon, skin) can prevent a joint from moving passively through its full range [2]. Development of a joint contracture can therefore occur due to a variety of etiologies, for example trauma [3], spasticity [4], burns [5], and immobility [1,158], that affect one or more of these structures. Degenerative diseases of the joint, such as rheumatoid arthritis (RA) and OA can alter bony and soft tissue anatomy, leading to contracture [5,6,7,8].

Contracture of the knee

A knee flexion contracture is a limitation in knee extension, often defined as 6° or more [2,9,10,11]. In the fully extended knee, the joint can bear weight and remain stable without muscular action. This relieves the knee musculature from using energy to stabilize the desired position. In patients with knee flexion contractures, the neutral position cannot be achieved, leading to a constant demand on the knee extensors during standing or ambulation [13]. The percentage of maximum quadriceps force required for stability is estimated to increase from 15% at 5° contracture, to 22% at 15°, and to 50% at 30° [13]. Walking is slow and abnormally tiring for these patients as there is a decrease in stride length and increased oxygen uptake compared to normal [12]. Flexion contractures also have a negative impact on standing balance [14], which increases the likelihood of falls [15]. Patients may limp due to a functional leg length discrepancy and/or require a gait aid. Active individuals may be limited in high-end activities, such as running, if they develop a contracture.

Knee contracture can be caused by numerous diseases, some of which are genetically-determined. As such, there are a vast number of genetic abnormalities that may be associated with joint contracture [16]. The timing of onset of joint contracture also depends on which genes are involved, and the severity of disease. Arthrogryposis multiplex congenita, a group of nonprogressive conditions characterized by multiple joint contractures at birth [17], occurs largely secondary to fetal akinesia, and has been

associated with numerous identified genetic abnormalities [18]. Neuromuscular diseases commonly lead to joint contracture. These include Duchenne and Becker muscular dystrophy (defects in the *dystrophin* gene [19]), limb-girdle muscular dystrophies (defects in calpain-3, dysferlin, and the sarcoglycan complex [19,20]), Bethlem myopathy (*collagen VI* [21]), and Emery-Dreifuss muscular dystrophy (*emerin*) [19]. Often, contracture develops earlier in more severe forms of neuromuscular disease as muscular weakness leads to imbalance of agonist-antagonist muscle pairs and patients no longer have the ability to actively move a joint through its full range [22].

Contractures may occur following trauma. Hildebrand *et al.* examined the joint capsule of patients with chronic elbow contractures post-fracture. Changes in gene expression were identified using reverse transcription-polymerase chain reaction (RT-PCR) [23]. These include an increase in collagen types I, III, and V, biglycan, a number of matrix metalloproteinases (MMPs) and a decrease in tissue inhibitors of MMPs (TIMPs). This could reflect an environment with high matrix turnover rates [23]. The same group showed that mRNA levels were increased for transforming growth factor-β1 (TGF- β1), connective tissue growth factor, and α-smooth muscle actin (α-SMA) in both human and rabbit post-traumatic models [24]. These factors have been shown to increase the number of myofibroblasts (MFs), a differentiated form of fibroblast that contributes to capsular contraction [25,26].

Regardless of the etiology, the first line of treatment for established joint contractures is rehabilitation, including modalities, stretching, bracing, serial casting and ROM exercises [1]. Although progress in the recovery of the loss ROM can be made using these conservative methods, adequate recovery may not be achieved and surgery becomes the next line of treatment [1]. Because knee flexion contractures occur commonly in OA [10,28], TKA allows for access to capsule tissue in order to study the pathophysiology of joint contractures.

Animal models to study immobility-induced joint contractures

The immobilized rat joint has been used as a model to study the pathophysiology of joint contractures. The knee is immobilized at 135° from full extension and the ROM measured over the time course of a 32-week period (29,30). Results indicated a gradual loss of ROM during the first 8 weeks of immobility and demonstrated that articular structures, including the posterior knee capsule, were important factors limiting knee joint mobility (29,30). A rat study examining the reversibility of contractures following 8 weeks of immobilization showed that the posterior capsule was the main contributor to contracture, and that 4 weeks of remobilization failed to restore full joint range of motion [31]. Studies from different groups examining ROM in different animal models following immobilization also showed that contractures do not fully resolve following remobilization [32-37]. From those observations, the authors searched for molecular mechanisms leading to capsule stiffness.

Evidence for a genetic contribution to immobilization-induced contractures was obtained from experiments using different rat strains under the same environmental conditions. Dark Agouti and Fisher 344 strains developed more severe contractures than Augustus Copenhagen Irish and Brown Norway strains [38]. These results suggested that intrinsic genetic factors participated in the process leading to joint contracture. Immunohistochemistry (IHC) studies of immobilized rat knee capsule and cartilage showed that cyclooxygenase (Cox)-1 protein levels were lower in synoviocytes of the anterior capsule compared with rats receiving sham surgery. Cox-2 protein levels were lower in synoviocytes of the posterior capsule but higher in chondrocytes at the anterior, posterior, and opposed aspect of the tibia compared to non-operated controls [39]. This suggested that chondrocytic isoenzymes of Cox are important in cartilage degradation of contractured joints. The same group found higher type I collagen levels in immobilized legs than in sham-operated legs in the anterior and posterior subintima, and lower type III collagen levels than in sham-operated legs in the anterior and posterior synovial intima, suggesting that the contracture process was caused by fibrosis, not new tissue proliferation, distinguishing this process from granuloma, scar tissue and the pannus of inflammatory arthritis [15]. Using differential display PCR (ddPCR), rat knee chondrocytes were found

to have increased expression of *Chitinase 3-like Protein 1* mRNA (an inhibitor of cellular responses to *tumour necrosis factor-α* (*TNF-α*) and *interleukin-1* (*IL-1*) that may delay cartilage degradation) [40], *myeloid cell leukemia sequence 1* (*Mcl-1*) mRNA (related to the anti-apoptotic protein *B-cell lymphoma 2* (*Bcl-2*), which may have an anti-apoptotic role) [41], and *prothrombin* mRNA (a precursor to *thrombin*, which has been shown to maintain an inflammatory state in rheumatoid arthritis synovium, and participates directly in degradation of the cartilage matrix by inducing the release of proteoglycans) [42].

Taken together, our current knowledge of contractures suggests a complex interplay between a number of intracellular and extracellular processes. A number of important pathways including inflammation, matrix protein degradation and remodelling, fibrosis, and apoptosis have been identified. The underlying pathogenesis of contracture therefore appears to be multifactorial. Further research is necessary to fully decipher the mechanisms leading to joint contracture, however the multiple mechanisms imply a role for both genetic and/or environmental factors.

Osteoarthritis

OA is by far the most common joint disorder, one of the most common chronic diseases in the elderly, and a leading cause of disability [43]. The prevalence of symptomatic knee OA increases with age and affects roughly 10% of people over the age of 63 [44].

There are a number of risk factors associated with the development of OA. These include older age, female gender, elevated body mass index (BMI), hormonal status, prior trauma, excess physical activity, repetitive joint movements, and abnormal joint loading (e.g. from developmental abnormalities or acquired, altered joint architecture) [45,46]. There is also a strong genetic component to OA heritability [47]. Twin studies have shown a heritability of about 58% for radiographic hip OA [48], and 39% for knee OA [47]. There is a racial predisposition to acquiring OA at different joints [45,46]. Studies to date have found that the genetic component likely involves small contributions from a large

number of genes, and that no one gene stands out as a major contributor across all races [47,49].

Linkage analysis has identified some genes contributing to OA development including *deiodinase, iodothyronine type 2* (*DIO2;*responsible for the local bioavailability of thyroid hormone in specific tissues, including the growth plate) [50], *acidic (leucine-rich) nuclear phosphoprotein 32 family, member A* (*ANP32A*; encodes a tumor suppressor molecule that plays a regulatory role in apoptosis) [47], and *growth differentiation factor 5* (*GDF5*; a gene involved in bone development and joint maintenance) [51]. *Peroxisome proliferator-activated receptor gamma* (*PPARγ*; a transcription factor that plays important roles in lipid homeostasis, epidermal maturation, skin wound healing, and brain development [52] has been implicated in OA). Treatment of OA chondrocytes with troglitazone, a PPARγ agonist, conferred a chondroprotective effect [52-54]. Another transcription factor, Sox9, has been identified as a potential therapeutic target in OA. Transfection of OA chondrocytes *in vitro* with a recombinant adeno-associated virus (rAAV) SOX9 vector increased expression levels and synthesis of proteoglycans and type II collagen in a dose-dependent manner [55]. As with contracture, development of OA appears to be multifactorial with a complex interplay between different mechanisms.

Microarray analysis has been used to examine changes in gene expression associated with OA. Using a commercial cDNA microarray for 1185 genes, Aigner *et al.* examined articular cartilage in patients with advanced OA and compared them to normal controls [154,155]. They showed an increase in the expression of *MMPs* 1, 8 and 13 and *collagens* 1, 2, 3 and 6 in the late OA group, likely representing the increase in matrix turnover seen in advanced disease [154]. Kato *et al*. used a custom cDNA microarray of 3265 selected genes to examine differential gene expression in the synovium of patients with OA compared to RA and trauma controls [153]. They found 21 differentially expressed genes from several functional groups including enzyme/enzyme enhancer/inhibitor, ECM, and receptor signalling proteins. Changes in the expression of several of these genes, including *protein phosphatase 2, regulatory subunit B', gamma, exostosin 1, heparan sulfate 6-O-sulfotransferase 1,* and *glutathione S-transferase theta 1*, corresponded to the radiologic severity of OA [153]. OA genetic markers have been

identified from fibroblast-like synoviocytes cultured from the synovium of patients with severe OA undergoing TKA, including *clusterin*, *sarcoglycan-g*, *G protein-coupled receptor 64*, *POU class 3 homeobox 3*, PPARγ, and *tripartite motif containing 2* [156]. Microarray has also been used to look at gene expression at the pathway level [56-59]. The first comprehensive gene expression analysis of human OA cartilage compared to control cartilage from donors lacking macroscopic and microscopic signs of OA using recently developed microarrays containing the whole human genome was published in 2010 [56]. Upregulated gene expression patterns were found in a number of pathways including angiogenesis, apoptosis, cell adhesion, cytoskeleton ossification, proteolysis, differentiation and ECM production, and cytokines [56]. An *in vitro* model of increasing shear forces in chondrocytes in culture recapitulated the gene expression patterns of OA including genes involved in ECM/matrix degradation, cell growth/differentiation, inflammation, and apoptosis [57].

The Joint Capsule in Contracture and Osteoarthritis

In OA, there are numerous structures which can contribute to the development of a flexion contracture of the knee including shortened muscle, ligament, or capsule, and bony osteophytes [2]. Knee flexion contractures are often discovered towards the end-stage of the disease as their knee ROM is measured pre-operatively for TKA. At this stage it is not possible to determine which structure was the primary cause of the contracture. At this point however, many of these structures, including the joint capsule, will contribute to the contracture [2]. The knee joint capsule provides structural stability to the joint. The capsule is essential in maintaining joint function and homeostasis and is altered by both joint contracture [45,22,25,26] and OA [6-8]. In contractures secondary to immobility using a rat model, there is a decrease in synovial intimal length of the posterior capsule, with a corresponding reduction in synoviocyte proliferation [60,62]. There is an increase in type I collagen in the posterior synovial intima and subintima [61]. This suggests a shortening and fibrosis of the posterior capsule which could potentially contribute to the limitation in joint range of motion (ROM). The contribution of the capsule to ROM limitation likely increases as the contracture becomes more chronic [61].

In OA the synovium becomes edematous with microvascular congestion and a mild inflammatory reaction [63]. Synoviocytes proliferate and macrophages migrate and adhere to the synovial lining [64]. In more advanced cases, the proliferation of synoviocytes can resemble the pannus seen in inflammatory arthritic conditions such as RA [63]. Scattered lymphocytes and perivascular lymphoid aggregates may arise. Increased edema leads to persistent synovial effusions which can distort the capsule architecture thereby disrupting its supporting and nourishing functions [63-64]. External to the subintima, increased collagen fiber formation leads to more widespread fibrosis and inflammation [63]. Due to fluctuating intra-articular fluid volumes, the capsule and supporting ligaments can become lax, reducing articular support and facilitating incremental joint injury [63]. In the knee joint, as cartilage damage progresses, the joint may be held in a flexed position, as this is less painful. Over time the posterior capsule can shorten resulting in a contracture.

Surgical arthroplasty to treat end-stage knee osteoarthritis: The impact of knee joint contracture

Total knee arthroplasty (TKA) is commonly used to treat end-stage OA. A significant percentage of patients eligible for TKA present with a knee flexion contracture. In a study of over 5600 knees for TKA, 93% of which had OA, more than 1/3 of patients had a flexion contracture. Of these, 8.5% were considered severe (>20°) [10]. In smaller studies, Tanzer *et al.* [28] found that 3 of 24 knees had contracture, and Tew *et al.* [2] found contractures in almost half of 219 knees. Those with flexion contractures are more likely to have increased pain and worse functional outcome post-operatively [10,68]. In fact, 2 studies have demonstrated that more severe contractures are highly associated with worse post-operative outcome after knee arthroplasty[10,68].

Patient demographic factors associated with knee contractures in OA prior to TKA have not been well characterized. A few studies of degenerated knees with contracture have examined patient demographics, but have been inconclusive at finding factors predictive of range of motion limitation [65-68]. Anouchi *et al.*[68] found decreased knee ROM post-TKA in patients with an elevated BMI at 1 year, but not at 2 years. Keeney *et al.* found no distinguishing demographics in patients undergoing revision TKA for painful

ROM [65]. Laskin *et al.* anecdotally reported that patients with truncal obesity and heavy legs had difficulty regaining full ROM after surgery. Ritter *et al*. suggested that decreased preoperative extension, preoperative tibiofemoral alignment, type of posterior release, gender and age were likely to be related to the postoperative extension [69].

Joint contractures are associated with reduced function, increased risk of falls, and poorer outcome post-TKA. Despite common mutual occurrence, little is known about the interaction between OA and joint contractures. OA is therefore a good model in which to study contracture for 3 reasons: the functional impact, the high prevalence of both conditions, and accessibility to capsule tissue during TKA, a commonly performed surgery in most major health centers. While both pathologic conditions produced specific gene expression changes, no data exist that compared gene expression of patients with OA and contractures to those with OA and no contractures. Effective prevention and treatments of knee joint contractures in OA may have practice-changing impacts: they could improve the life of a large number of patients suffering from a combination of OA and knee joint contractures and improve the outcomes post-arthroplasty surgery. Identifying risk factors for joint contractures in OA could alter OA severity classification and OA functional consequences. Characterization of histologic and genetic differences in OA knee capsule with and without contracture can contribute to our understanding of the pathophysiology of the two diseases and help direct research and treatment.

Our goal was to find differentiating factors between patients with end-stage knee OA that had a joint contracture compared with those that did not have a joint contracture. We tested 3 hypotheses: 1) Demographic factors including increased OA severity, elevated BMI and increased duration of OA are associated with patients with end-stage knee OA and contracture compared to those without contracture. 2) there is an increase in non-adipose tissue and decrease in adipose and synovial tissues in posterior knee capsules of patients with OA and contracture compared to those with OA without contracture. 3) there is an increase in pro-fibrotic gene expression including collagen-1 and TGF-β in the posterior knee capsule of patients with severe OA with contracture compared to those without contracture. In order to test these hypotheses, we 1) studied the demographics of patients with end-stage OA with and without knee contracture at the time they underwent

TKA in a case-control design, 2) performed a histologic measure of the fibrous, synovial and adipose content of their knee capsule harvested during TKA using light microscopy, and 3) examined differential gene expression of the same tissues in same patients, using DNA microarray followed by PCR and IHC.

Materials and Methods

Patient Recruitment and Data Collection

Patients with severe OA were either recruited during their preoperative assessment for TKA in the outpatient clinic, or on the day of their TKA, prior to their surgery in the preoperative assessment area of The Ottawa Hospital, General site (TOH), in Ottawa, Ontario, Canada. For patients seen in the preoperative clinic, the listings for patients for TKA were obtained by our research staff one or two days prior to the patient's visit. A chart review was performed using the medical record provided in clinic, the surgeon's medical record, and the hospital electronic medical record. If the patient met the inclusion criteria and did not meet exclusion criteria for our study, then the date of their surgery was recorded. Consent for participation, patient demographics, and measurements of knee range of motion (ROM) were obtained while the patient was in clinic. The chart was then flagged to let staff know that the patient was included in the study. Knee capsule tissue was obtained during surgery. Operating room (OR) staff received a phone call from our research staff on the day of surgery to remind them to collect the tissue. Sample tubes containing RNAlater® solution and instructions for tissue collection were placed on the chart on the day of surgery.

Patients recruited on the day of TKA were seen 1 to 2 hours prior to their surgery in the Surgical Day Care Unit at TOH. Consent, patient data, and knee joint ROM were obtained as above. The chart was then flagged and sample collection tubes containing RNAlater® solution and capsule harvesting instructions were placed on the chart. The OR staff, including the surgeon, were contacted to inform them of collecting the tissue.

Joint Range of Motion

Prior to TKA, the patient was placed in the supine position with the knee in extension. The hips were positioned in 0° of extension, abduction, or adduction and a towel roll or folded sheet was placed under the calcaneus to allow the knee to extend as much as possible (this may have required slight hip flexion). The femur was stabilized to

prevent rotation, abduction, or adduction of the hip. To test the motion of the knee, the subject's ankle was held in one hand and the thigh moved with the other hand. The subject's thigh was moved to 90° of hip flexion and the knee moved into flexion. The end ROM in knee flexion occurred when manual force could not overcome resistance.

Once flexion ROM was established, the subject's leg was placed back in the position with the hip to 0° of extension, abduction, or adduction and the knee in extension (there may have been some hip flexion if foot needed to be elevated to get maximum knee extension, i.e. if a hip flexion contracture was present). The greater trochanter (GT), the lateral condyle of the femur, the fibular head, and the lateral malleolus were palpated and landmarked. Each of these structures was marked with a pen. To align the goniometer, the fulcrum was centered over the lateral condyle of the femur. The proximal arm was aligned with the lateral midline of the femur, using the greater trochanter as reference. The distal arm was aligned with the lateral malleolus and fibular head for reference. The angle marked on the goniometer was recorded – this was the angle of extension. Zero degrees was noted as full extension. Notation for a 7° flexion contracture read "maximum knee extension = 7°. If there was hyperextension (recurvatum) present, the angular measurement was followed with the words "of hyperextension". For example a patient with 5° of hyperextension would be written as "maximum knee extension = 5° of hyperextension". A lack of extension greater than 5° was considered a flexion contracture.

In order to measure the maximum angle of knee flexion, the hip was returned to the 90° flexed position with the knee flexed until resistance was felt (as above). While stabilizing the lower extremity, the GT was re-marked (as the initial mark shifted with the skin moving over the GT). The lateral femoral condyle, fibular head, and lateral malleolus were already marked. The alignment and positioning of the goniometer was performed using the same landmarks as noted above. The angle on the goniometer was recorded – this was the angle of flexion. The same process was repeated for the contralateral leg.

All but one measurement were performed by one of two research assistants from the Orthopedic Department trained by the author. A first research assistant recruited and measured 4 patients, one measurement was made by the author, and 7 patients were recruited and measured by the second research assistant. The method we used to measure joint ROM displayed high inter rater reliability [9].

Radiographic Severity of OA

Radiographic severity was graded based on the Kellgren and Lawrence criteria [159]. Severity was graded by 2 clinicians. In the event that there was disagreement, the grade assigned by the more experienced clinician was kept. The criteria are shown below:

Grade 1	Doubtful narrowing of joint space and possible osteophytic lipping
Grade 2	Definite osteophytes and possible narrowing of joint space
Grade 3	Moderate multiple osteophytes, definite narrowing of joints space, some sclerosis and possible deformity of bone ends
Grade 4	Large osteophytes, marked narrowing of joint space, severe sclerosis and definite deformity of bone ends

Knee Alignment (Varus and Valgus) Measurements

Varus and valgus measurements were determined for each subject when an appropriate x-ray was available and the Contracture group was compared to the No Contracture group. Because full-length lower extremity standing x-rays were not available, a method using the tibial spines as a reference point was selected (161,162). Knee alignment was determined by anatomic axis, using knee radiographs performed in the standing position. The femoral anatomic axis was determined by drawing a line from the centre of the tibial spines to a point 10 cm above the tibial spines, midway between the medial and lateral femoral surfaces. The tibial anatomic axis was determined by drawing a line from the centre of the tibial spines to a point 10 cm below the tibial spines, midway between the medial and lateral tibial surfaces. Varus alignment was indicated by values < 180° and valgus alignment is indicated by values > 180°. The radiographer was blinded to subject grouping for all measurements. Statistical comparison between groups was done using the Mann Whitney U test in SPSS 16.0.

Determining Presence of Osteophytes

The presence of osteophytes in either the posterior compartment of the knee or inter-condylar femoral notch was determined for the 12 subjects included in the microarray analysis (see below). The Contracture group was compared to the No Contracture group.

There was variability in the X-ray views available for each subject (e.g. some subjects did not have skyline views). All available views were used for each subject to maximize accuracy of osteophyte detection. The radiographer was blinded to subject grouping for all x-rays. Statistical comparison between groups was tested using the chi squared test calculated manually. The No contracture group values were used as the "expected" values.

Tissue Collection and Storage

On surgery day, OR staff were reminded to collect capsule tissue. A bag containing 4 vials of RNAlater® solution and instructions for tissue collection were placed at the front of the chart. The vials were labelled as: Posterior medial, Posterior lateral, and Suprapatellar, corresponding to the location of the capsule. The fourth vial was included for any extra sample or if one tube was damaged or spilled. During TKA surgery, capsule samples no greater than 0.5cm in diameter were collected by the surgeon and completely submersed in the test tubes. Once successfully collected, OR staff contacted the laboratory staff for pickup. In the laboratory, the specimen was quickly divided into 4 pieces: 1 for histology, and 3 for RNA extraction. The 3 samples for RNA extraction were placed in separate tubes, each containing RNAlater® solution. Each sample was submersed completely and stored for 24 hours at 4° C. No sample waited for more than a few hours before being refrigerated. After the 24-hour incubation at 4°C, samples were transferred to storage at -80° C. The sample destined for histology was submersed in 10% buffered formalin for tissue preparation at a later date.

Total RNA Isolation

Capsule samples were removed from storage at -80° C and allowed to thaw on ice. Once samples were thawed, sample homogenization was performed using a mortar and pestle and measuring scoop. This equipment was first washed thoroughly with soap and water, and then dried. Equipment was then thoroughly soaked with 100% ethanol. Ethanol was dried rapidly by ignition. Before placing a capsule sample into the mortar, liquid nitrogen was poured into the mortar. The tissue sample was then dropped into the liquid nitrogen, and then pulverized with the pestle. More liquid nitrogen was added during

homogenization if the sample was not completely homogenized after the first volume and impacting was repeated. Homogenate was scooped from the mortar using the measuring scoop. The homogenate was then transferred into an Eppendorf tube containing 1mL of Trizol solution and submerged quickly by tapping the tube or closing the tube and inverting it. Tubes were then lightly shaken by hand to separate homogenate aggregates.

Tubes were allowed to sit at room temperature for 5 minutes. Following this, they were placed in a Labnet Hermle 7233 MK-2 centrifuge and spun for 10 minutes at 12,000g at 4° C in order to separate total RNA from gross debris and large DNA fragments. Three hundred µL of chloroform was then added to each Eppendorf tube, and tubes were shaken vigorously by hand for 15 seconds. Tubes were left at room temperature for 3 minutes. Tubes were then centrifuged for 15 minutes at 12,000g at 4° C. The upper aqueous phase containing total RNA was then transferred to a fresh tube. Five hundred µL of isopropyl alcohol was added to the tube and shaken gently. The tube was then allowed to stand for 10 minutes at room temperature. The sample was then centrifuged for 10 minutes at 12,000g at 4° C. This caused the RNA to precipitate in a small gel-like pellet at the bottom of the tube. The supernatant was removed and the pellet was washed with 1mL of 75% ethanol. The tube was then centrifuged for 5 minutes at 7,500g at 4° C. The supernatant was removed and the tube was left to dry at room temperature for 10 minutes. The pellet was then resuspended in 100µL of RNAse-free water by gentle pipetting and incubation for 10 minutes at 60° C.

In order to remove non-RNA contaminants, the re-suspended RNA was applied to the Qiagen RNeasy mini kit column according to the manufacturer. The full protocol can be found at *http://www.qiagen.com/products/rnastabilizationpurification/rneasysystem/rneasymini.aspx#Tabs=t2* under the resources tab. The detailed protocol used in this study is shown below.

RNA Cleanup

Buffer RLT and RPE are commercial product manufactured by Qiagen. Ten µL of beta-mercaptoethanol were added to buffer RLT per 1mL of buffer RLT. This could be

used for 1 month. Ethanol was added to buffer RPE prior to use as per the manufacturer instructions.

Three hundred and fifty µL Buffer RLT was added to the 100µL RNA sample and mixed well. Two hundred and fifty µL of 100% ethanol was added to the diluted RNA, and mixed by pipetting. The sample was then transferred to an RNeasy Mini spin column placed in a 2 ml collection tube. All centrifugation was done using the Eppendorf Centrifuge 5415C. Samples were centrifuged for 15 s at 8,000g. The flow-through was discarded. After centrifugation, the RNeasy spin column was removed carefully from the collection tube so that the column did not contact the flow-through.

Five hundred µL Buffer RPE was then added to the RNeasy spin column. This was centrifuged for 15 s at 8,000g (10,000 rpm) to wash the spin column membrane. The flow-through was discarded. The collection tube was reused for the next step. Five hundred µL Buffer RPE was added to the RNeasy spin column and the column was centrifuged for 2 min at 8,000g (10,000 rpm) to wash the spin column membrane. After centrifugation, the RNeasy spin column was carefully removed from the collection tube so that the column did not contact the flow-through.

The RNeasy spin column was placed in a new 1.5 mL collection tube. Fifty µL RNase-free water was added directly to the spin column membrane and the tube was centrifuged for 1 min at 8,000g (10,000 rpm) to elute the RNA. For some samples, a further 50µL of RNase-free water was added to the column and the column was re-centrifuged for 1 min at 8,000g (10,000 rpm) to elute any RNA remaining on the column membrane for a total final volume of 100µL added. For some samples, the eluate from the previous step was replaced on the membrane and re-centrifuged for 1 min at 8,000g (10,000 rpm) to elute any RNA remaining on the column membrane for a total final volume of 50µL. Samples were then stored at -80° C and collection of all samples completed before performing RNA expression analysis.

Extracted RNA Quality Assessment

Extracted RNA quality was assessed using the Experion™ RNA StdSens Analysis kit. The full manual can be found at

http://www.genmall.com.tw/products/HB/Experion%20RNA%20%20StdSens%20Analysis%20Kit.pdf and the details of the method used in this study are described below:

All kit reagents (except the RNA ladder) including RNA gel, RNA gel stain, and loading buffer were equilibrated to room temperature (about 15–20 minutes). Kit reagents were vortexed and briefly centrifuged before use to ensure homogenous solutions. RNA stain and gel-stain solution were protected from light during experiments as some components in these reagents are light sensitive. Prior to use, the RNA ladder and RNA samples were allowed to thaw on ice, then briefly at room temperature, then heat-denatured for 2 minutes at 70° C immediately before use. All chips were run within 5 minutes of loading all samples.

The Experion Automated Electrophoresis Station, which is designed to analyze the samples loaded into the gene chip, requires cleaning of its electrodes prior to use. To clean electrodes before a run a cleaning chip was filled with 800 µL Experion electrode cleaner. No air bubbles were trapped in the reservoir (the side of the cleaning chip was gently tapped to remove any bubbles). The cleaning chip was left in the instrument for 2 minutes. A separate cleaning chip was then filled with 800 µL of Diethylpyrocarbonate (DEPC)-treated water. DEPC inactivates the RNases by the covalent modifications of their histidine residues [71]. If the cleaning chip was being used for the first time, the chip was treated with the Experion electrode cleaner to remove any RNase contamination within the chip prior to use. This was done by completely filling the new cleaning chip with Experion electrode cleaner, allowing it to sit for 5 minutes, discarding the solution, and then thoroughly rinsing the chip (4–5 times) with DEPC-treated water.

After using the cleaning reagent, the lid was opened and the cleaning chip containing the electrode cleaner was removed. It was then replaced with the chip containing the DEPC-treated water. The lid was closed and the chip left in the instrument for 5 minutes to rinse the electrodes. The DEPC-treated water in the DEPC water chip was replaced and the rinse step repeated for 60 seconds. The DEPC water chip was then removed from the instrument. The lid was left open for 60 seconds allowing for any water remaining on the electrodes to evaporate.

To prepare new gel stain, 600 µL RNA gel (green cap) was pipetted into a spin filter tube then centrifuged in the Labnet Hermle 7233 MK-2 centrifuge at 1,500g for 10-15 minutes. It was confirmed that all of the gel had passed through the filter, then the filter was discarded. It was recommended that the filtered gel could then be used for 4 weeks of preparation before requiring re-filter however on some occasions up to 8 weeks after preparation were allowed to lapse. No performance errors were noted due to this.

Once the gel was filtered, 65 µL filtered gel was pipetted into an RNase-free microcentrifuge tube. One µL of RNA stain was then added to the tube and the solution was briefly vortexed. The resulting gel-stain (GS) solution was kept protected from light.

To prepare the samples and RNA ladder, the RNA ladder (red cap) was removed from storage and allowed to thaw on ice. The amount of RNA ladder required was 2µL as only 1 chip was run at a time. The RNA ladder was then pipetted into an RNase-free microcentrifuge tube. Samples were prepared by pipetting 3 µL of each RNA sample into RNase-free microcentrifuge tubes. The ladder and samples were denatured for 2 minutes at 70°C. The denatured ladder and samples were then cooled by immediately placing the tubes on ice for 5 minutes. The ladder and samples were then spun down in a microcentrifuge (Qualitron DW-41N-45) for 3–5 seconds and stored on ice until used.

To prime the Experion RNA StdSens chip it was first removed from its packaging, then placed on a clean flat surface that had been soaked in 100% Ethanol, then allowed to dry. With the chip on this clean surface, 9 µl filtered gel-stain solution was pipetted into the lower well labeled GS (white font). The tip of the pipet was inserted vertically and to the bottom of the well when dispensing. Care was taken not to expel air at the end of the pipetting step. Bubbles were dislodged at the bottom with a clean pipet tip. The chip was then placed on the priming station and the priming station lid was closed. The pressure was set to B and the time setting to 1, as specified by the alphanumeric code on the chip. The Start button on the chip primer was then pressed. Complete priming required approximately 30 seconds. An audible signal indicated that priming was complete, and a "Ready" message was displayed. Once the chip was removed, it was turned over and inspected to ensure the microchannels did not have air bubbles in them.

The chip was then placed on the same clean surface as above for loading samples. Nine µL of the gel-stain solution were pipetted into the upper well labeled GS (dark font). Nine µL of filtered gel were then pipetted into the well labeled G. Five µL of the loading buffer (yellow cap) were pipetted in each sample well (1–12) and the ladder well, labeled L. A new pipet tip was used for each delivery to prevent contamination of the loading buffer stock. It was ensured that the pipet tip was centered and positioned vertically all the way to the bottom of the well to avoid introducing bubbles into the bottom of the wells. One µL of denatured RNA ladder was then pipetted into the well labeled L. One µL of each sample was pipetted into each of the 12 sample wells. If fewer than 12 samples were run, 1 µl of loading buffer was added to the unused sample well(s) to equalize the load volume. The chip was placed in the Experion vortex station and the vortexer was turned on. This operated for 60 seconds and then automatically shut off. The chip was removed when the vortexer stopped. The analysis run was started within 5 minutes of vortexing to prevent excessive evaporation and poor results or a chip performance error.

To run the RNA analysis, the Experion automated electrophoresis station was turned on by pushing the green button in the center of the front panel. The Experion software was then launched on the lab computer. The primed chip, which had been loaded with the samples as described above, was placed on the chip platform. With the software running, the following selections were made: New Run, then RNA StdSens protocol (Eukaryotic total RNA). The number of samples was selected then the Start button was clicked to begin the chip run. The analysis took about 30 minutes. When the chip run was complete, a "Run complete" message was displayed. The chip was removed from the electrophoresis station and disposed of. To prevent contamination of the electrodes, the chip was removed from the electrophoresis station immediately after the run. The electrodes were then cleaned.

To clean the electrodes after the run, the cleaning chip labeled DEPC water was filled with 800 µl DEPC-treated water. This chip was placed the cleaning chip on the instrument chip platform. The lid was then closed and the chip left for 60 seconds. The DEPC water chip was then removed, the electrodes allowed to dry for 60 seconds, and the lid closed.

In order to assess the quality of the RNA samples, the data from the StdSens Analysis software was examined. Data output from the software included a virtual gel and fluorescence vs. time graphs for the RNA ladder and each sample. Fluorescence peaks corresponded to higher concentrations of RNA at a specific molecular weight (RNA of similar weight migrated through the gel at a similar rate, and was detected by the StdSens analyzer). The 3 major peaks from left to right included the reference peak (provided in the Experion loading solutions), the 18S RNA peak, and the 28S RNA peak. Amount of degradation and impurity was determined using the 28S/18S ratio (a ratio greater than 1 is considered a high quality/low degradation sample as the 28S RNA tends to degrade the most rapidly). The RNA Quality Indicator (RQI) number was also used to assess the quality of RNA. The RQI measures RNA integrity by comparing the electropherogram of RNA samples to a series of standardized degraded RNA samples. This method returns a number between 1 (highly degraded) to 10 (intact RNA). For this study, the RQI values were interpreted as recommended by BioRad [BioRad tech note 5761]: 1-4 = highly degraded, 4-7 = moderate degradation, 8-10 = minimal degradation.

Microarray Hybridization

Gene expression was assessed by microarray analysis on all samples simultaneously. Adequate RNA samples, based on RNA degradation (previous section) were obtained from the posterior lateral or posterior medial knee capsules of 12 patients: 6 with severe OA and contracture, and 6 with severe OA without contracture. Genome-wide RNA expression was determined using the Illumina HumanHT-12 v4 BeadChip. A single chip allows analysis of 12 samples and contains 47,231 distinct probes representing the entire human genome and some transcript variants [70]. The direct hybridization assay of the RNA samples to the chip and gathering the data output from the chip were performed by the Génome Québec Innovation Centre at McGill University. The general protocol for hybridization is described in the following paragraph.

The integrity of the RNA sample was first determined using a similar protocol to that described above, however the Agilent technology was used to produce an RNA

integrity number (RIN) as opposed to the RQI provided by the BioRad software. The RIN was calculated based on a number of factors including total RNA ratio, height of 18S rRNA peak, ratio of fast-migrating RNAs to total area of electropherogram, and height of the lower marker. RIN output is between 1 (completely degraded) and 10 (intact RNA).

Once the RIN was determined, the hybridization assay workflow was initiated. RNA undergoes duplication using RT-PCR such that a first strand synthesis and second strand synthesis are performed using the Ambion Illumina TotalPrep RNA Amplification Kit [72,73]. The resulting cDNA was then isolated and underwent amplification using in vitro transcription using biotin-labeled oligonucleotides. The resulting biotin-labeled cRNA was then purified and quantified, then set on the chip for hybridization. The Illumina HumanHT-12 v4 BeadChip uses beads bound on one side to a glass chip, and bound on the other side by a short address sequence of RNA linked to a 50-base gene-specific probe. There is one probe per bead. Once hybridization was completed, the chip was washed and scanned using the Illumina BeadArray Reader. A digital image of the fluorescing probes was obtained and store as a .CEL file. The fluorescence intensity of each probe is generated using Illumina software. This provides a raw signal for each probe, representing raw signal for each gene.

Subject Matching

For our case-control design, contracture patients were matched 1:1 with an appropriate control using a points system. Control subjects who had more patient-related factors in common with contracture subjects scored more points. The control and contracture subject with the highest points were matched and included in the microarray analysis. Ordinal ranking of demographic factors was based on the demographic data we collected since no literature existed to guide this step. Priority was given to those characteristics which were found to be statistically significantly different or trended towards a difference in the demographics study described above (duration of OA, contracture of contralateral knee, BMI). The points system was assigned as follows: Duration of OA = 8 points; Contracture of contralateral knee = 7 points; BMI = 6 points;

Severity of OA = 5 points; Ethnicity = 4 points; Gender = 3 points; Age = 2 points; Prior joint Injection = 1 point.

Microarray Data Analysis

Data from the Illumina gene chip obtained as .CEL file were converted to a text files containing quantitative information for gene expression in a two-step process; first the intensity of hybridization to each probe is obtained and second, the probe intensity is associated to the corresponding genes. Those steps were conducted using the software FlexArray 1.5 and provided by Genome Quebec. Data analysis was performed using the data at the gene level. The data was analyzed using Flexarray 1.5, then later Flexarray 1.6 when it was released. Flexarray uses the freeware R program for statistics and for the conversion of hybridization intensities recorded as .CEL files to numerical values.

Data from the Illumina HumanHT-12 v4 BeadChip was imported into Flexarray. This displayed the raw signal for each gene for each patient sample. Samples were separated into 2 groups: "Contracture" and "No Contracture". The Raw Data was processed using the "lumi" data processing option. Background correction and normalization was performed using the Robust Multiarray Average (RMA) which uses intensity values transformed into log2 values [74]. Data transformation/Variance stabilization was performed using the Variance stabilization transformation unique to Illumina chips. Normalization was performed using quantile normalization. Once these were completed, relative, normalized, and summarized gene expression data was displayed for each patient. In order to compare gene expression between the 2 groups of patients, the empirical base (Wright and Simon) test was performed. This was initially done including all patients. A separate analysis using RMA background correction, log2 data transformation and Loess normalization was performed to confirm that differential expression of selected genes with a different statistical approach.

Different strategies for data analysis were conducted to explore factors contributing to variation of expression. Analysis included a strategy to identify patient samples that were outliers. This involved using the multivariate projection method of principle component analysis (PCA) provided by Flexarray. The largest factor (called “Component 1” by

Flexarray) separating patients in the PCA analysis was gender. Because there were 3 males and 9 females in our sample, the 3 males were excluded for a separate data analysis. With male samples excluded, the statistical analysis was conducted using a similar strategy as the one used when all samples were included (RMA, variance stabilization transformation, quantile normalization).

A final statistical analysis was performed removing the 2 greatest outliers for Component 1 (2 males). Taking advantage of the case-control nature of the subject matching, the corresponding matched subject was also removed from the analysis leaving 8 subject included in the analysis. This was performed to determine if the outliers and their matched subjects were influencing the results of the previous analyses. Because we could not determine which factors corresponded to the other major outlier factors in the PCA (called Components 2 and Components 3 in Flexarray), this analysis also allowed us to determine if our other matched factors that were felt to be significant (duration of OA, contracture of contraleteral knee, etc.) from the 4 removed subjects were having a strong effect on the analyses performed above.

For correlation calculations, microarray gene expression was done using data post-RMA, VST, QN, then compared to the degree of flexion contracture. Correlations were calculated using SPSS 16.0. Both the Pearson (for parametric data) and Spearman (for non-parametric data) analyses were included.

Histology Sample Processing

The capsule tissue used for each subject and the area of the capsule from which it was collected is shown below:

Sample and Capsule Region Used:

H21 - posteromedial

H43 - posteromedial

H50 - posterolateral

H51 - posterolateral

H53 - Posteromedial

H54 - Posterolateral

H15 - lateral capsule

H25 - posteromedial

H32 - posterior medial

H33 - posteromedial

H41 - posterolateral

H55 – posterolateral

Capsule samples were kept in formalin for 24 hours prior to dehydration in 60% ethanol. Following dehydration, samples were processed using a standard histology protocol:

Step 1: 60% Ethanol; Step 2: 70% Ethanol; Step 3: 80% Ethanol; Step 4: 95% Ethanol; Steps 5-8: 100% Ethanol; Step 9-10: Toluene; Step 11-15: Paraplast plus wax 58. Each step lasted 1 hour. Temperature for steps 1-8 = 40°C, steps 9-10 = 45°C, steps 11-14 = 58°C. Gentle agitation was applied during each step. All steps were carried out in the Triangle Biomedical Sciences ATP1 - Automatic Tissue Processor.

Following sample processing, paraffin-embedded samples were cut into 5μm sections using the Leica Jung RM2035 microtome. Once sectioned, samples were stained with hematoxylin (Harris formula, Surgipath) and eosin (eosin Y), then visualized with the Olympus BH-2 light microscope. Digital images were obtained using the Marlin F080C digital camera (Allied Vision Technologies) mounted on the photo tube of the microscope and magnified using a 2.5X lens, in addition to the objective lens. Camera software was AVT Smartview 1.5.1.

Light settings for photos were as follows: For all images a red spectrum light filter was placed over the field lens. For images taken with the 1X objective lens, the field

diaphragm was opened and the intensity of the light source increased until the desired lighting was achieved, without using the light condenser. For images taken using the 10X, 20X, and 40X objective lens, the field diaphragm, the light condenser and light source intensity were optimized.

Histological Analysis

Histological digital images were described based on the proportion of "adipose", "non-adipose", and "synovial" tissues. Synovium, blood vessels, and other non-fibrous and non-adipose tissue were grouped with the "non-adipose" proportion. The total area of synovial tissue and synovial thickness were also described. In order to measure proportional area of each type of tissue within the entire tissue sample, digital images were taken using the 1X objective lens. If the entire sample did not fit in the visualized field, additional photos were taken so that the entire sample was imaged, without overlapping any areas. Samples were then digitally formatted for analysis of tissue proportions. Digital formatting consisted of removal of non-tissue background (mainly glass). This was done using Adobe Photoshop CS4. The Rectangle Marquee, Quick Selection, and Eraser tools were used at varying digital magnifications so that as much background could be removed as possible. Images were then saved as JPG files and opened using ImageJ software.

Colour files were converted to RGB stacks in ImageJ. For determination of adipose and non-adipose proportions, the "green" window was selected. For synovial area, the red window was selected. If further non-tissue background removal was necessary, it was done in ImageJ using the Rectangle, Wand, and Eraser tools. In order to differentiate non-adipose from adipose tissue, the "Adjust threshold" tool was used. Threshold adjustments between 173 and 222 were used to highlight fibrous tissue. The total area of the tissue sample was measured, and the percent adipose was calculated based on the remainder after subtraction of the non-adipose tissue area.

In order to determine synovial area, digital images were digitally magnified on the computer using CorelDraw and compared to concurrently, equally magnified images under the microscope using the 10X objective lens (25X total magnification). Using the microscope was necessary as the resolution of the digital photo at that magnification (from the image obtained using the 1X objective lens) was too low to distinguish synovial from

non-synovial cells. The two images were compared side-by-side at the same region of the tissue on the same monitor. By using the microscope image, it was possible to determine which areas of the digital image were synovial cells. These areas were coloured over in black on the digital image using the paintbrush tool. Once the entire image had been examined and coloured appropriately, the new file with black marking representing synovium was opened in ImageJ. Images were converted to RGB stack and the red window was used. Using the thresholding tool, the black area alone was highlighted (adjusted to a threshold between 80 and 100) and the area determined.

The image size scale (converting number of pixels to millimeters) was determined using a slide with a 1mm marker visualized under the 1X objective lens, and the number of pixels per mm were calculated using the "set scale" tool. This scale was used for all slides examined under the 1X objective lens. Total area of digital image using this magnification was ($29.6mm^2$). Subsequent scales for the 20X and 40X objective lens were done in the same manner, but using 1/100 of a mm as reference.

The number of cells per high powered field (HPF) was determined using the 20X objective lens (50X total) for adipocytes (total area of digital image = $7.7 X10^{-2}mm^2$) and the 40X objective lens (100X total) for fibroblasts (total area of digital image = $1.9 X 10^{-2}mm^2$). Cells were counted manually using the "Cell Counter" ImageJ plugin. Fibroblasts were counted by their nuclei. If more than half of the nucleus of the same cell was included in the region of interest (ROI), it was included. Adipocytes were counted by the number of visible cells. If more than half of the entire cell was included in the ROI, it was included. Two random fields were used for each cell type when they were identified (some samples did not contain adipocytes) and the average number of cells for HPF were calculated.

Synovial thickness was determined by identifying areas of synovium at low magnification. These areas were then visualized at either 25X or 50X and the number of cell layers was counted manually.

Polymerase Chain Reaction

RT-PCR was performed to confirm microarray data by examining the relative expression of the 3 genes of interest (*CHAD, Sox9, Cyr61*) between tissue samples. Beta-actin was used as the internal control. Template RNA was of the same origin as samples

used for the microarray experiments. RT-PCR was carried out using the Invitrogen Superscript™ One-Step RT-PCR with Platinum® Taq. Reaction mixture components were as outlined by the manufacturer for CHAD and Cyr61: 25 µL of 2X reaction mix, 2 µL Template RNA, 1 µL sense primer, 1 µL antisense primer, 1 µL RT/Platinum *Taq* mix, autoclaved distilled water to final volume of 50 µL. For Sox-9, only 0.8µL of actin template was used in order to more closely equalize product intensity for easier comparison. Actin primers and primers for the gene of interest were placed in the same tube.

Primers were designed for CHAD, Sox-9, and Cyr61 using the Invitrogen Oligoperfect™ free online primer designer (http://www.invitrogen.com/site/us/en/home/Products-and-Services/Product-Types/Primers-Oligos-Nucleotides/invitrogen-custom-dna-oligos/Primer-Design-Tools.html). Actin primers were already available in our lab. Primers were designed to amplify exon DNA only. The sequences of the primers used are shown in the table below:

Primer Pair	**Primer Sequence**	**Predicted Product Length (base pair)**
β-Actin forward primer	GCCAACCGCGAGAAGATGACC	300
β-Actin reverse primer	CTCCTTAATGTCACGCACGATTTC	
CHAD forward primer	CTCCACTACCAACCCAGCTC	361
CHAD reverse primer	AGAAATTGCAGCATGGGAAG	
Sox9 forward primer	TGTGCCTCTCAGAACACCAG	422
Sox9 reverse primer	TCTGTGGCAGAAAACACTGC	
Cyr61 forward primer	GCAGCGTTTCCCTTCTACAG	477
Cyr61 reverse primer	TGCCCTCCCATTTACTTTTG	

The PCR conditions were as follow: cDNA synthesis and pre-denaturation - 1 cycle of 45°C for 30 minutes then 94°C for 2 minutes. PCR amplification - 35 cycles of denaturation 94°C for 15s, annealing at 55°C for 30s, extending at 72°C for 1 min. Final extension - 1 cycle of 72° for 10 minutes. Samples were then stored at 4°C until run on agarose gel.

Electrophoresis of PCR Products

PCR samples were resolved on 1% agarose gels. Gels were prepared using 55mL of Tris-EDTA buffer and 0.55g of pure agarose. This mixture was microwaved for 1 minute, then 1 μL of ethidium bromide was added and mixed in. Gels were pored and allowed to solidify at room temperature. RT-PCR samples were loaded in gel wells and electophoresis was performed by setting the voltage to 95. The fastest dye front was allowed to migrate about 3/4 of the way down the gel, then electrophoresis was stopped. Gels were then imaged using UV light in the Alpha Inotech Corp. Multi image light cabinet, which included a camera, and digital images were taken using the Alpha imaging software.

PCR Band Quantitation

Once digital images of PCR gels were obtained the images were opened using ImageJ software. In the toolbar, the "Analyze" tool was selected followed by "Gels" then "Plot lanes". A rectangular box was drawn around the bands of interest (actin, and the gene of interest) in the first lane, then "select first lane" was selected from the "Gels" tool. Subsequent lanes were selected using the "select next lane" tool under the "gels" tool. Once all lanes were selected, the "plot lanes" tool was selected. Downward peaks for actin and the gene of interest were plotted by ImageJ. The magnifying glass function was used to increase plot image size to 200%. The straight line tool was then used to demarcate the base of the intensity peak. Once all peaks were demarcated the want tracing tool was clicked over the actin peaks. ImageJ then produced a numerical value for the peak area. The "label peaks" tool in the "gels" tools was clicked. This gave the percentage proportion that each peak occupied in the total area of all peaks combined. The peak area and proportional percentage were then copied and pasted into Microsoft Excel 2010. The relative density of each peak was then calculated relative to the actin peak in lane 1 by dividing each sample percent total area by the percent total area of the peak in lane 1.

Next the straight line tool was used to demarcate the base of the gene of interest. If there were 2 peaks side by side (corresponding to two bands close to one-another on the gel), these were both included in the calculation for "control" samples, but not for "contracture" samples in order to reduce the undercounting of gene expression in the

"control" group. The wand tool was used to calculate the area of each peak and the "label peaks" in the "gels" tools was used to give the proportional percentage of each peak relative to the first peak. The relative density of each peak was calculated as for actin. In order to obtain the adjusted density relative to how much actin was in each sample lane, the relative density for each gene of interest was divided by the relative density for the actin band in its lane.

The adjusted density for each group (no contracture and contracture) was compared using SPSS 16.0 using a 2-tailed independent-samples student's t-test to give a final average expression for each group and a p-value. Expression was considered significantly different if $p < 0.05$.

Immunohistochemistry

Tissues from the same samples as used in the histologic analysis were examined for expression of protein products of our 3 genes of interest. Primary antibodies to Chondroadherin (CHAD), sex determining region Y-box 9 (Sox-9), and cysteine-rich, angiogenic inducer 61 (Cyr61), were purchased from Sigma Aldrich. All primary antibodies were from the Prestige Antibody^{R} collection of polyclonal, monospecific, affinity-isolated rabbit anti-human antibodies: Anti-CHAD: HPA018241, Anti-Sox-9: HPA001758, Anti-Cyr61: HPA029853.

Other reagents used for immunohistochemistry were purchased from Biocare Medical with the exception of the diaminobenzidine (DAB) which was purchased as a kit (Biogenex Liquid DAB Substrate Pack, Concentrated for use with peroxidase). These included the secondary polymer MACH 3 rabbit antibody detection system conjugated to horseradish peroxidase, Background Sniper, and Peroxidazed 1.

CHAD, Sox9 and Cyr61 IHC were performed as follows:

Five µm paraffin slices on slides were allowed to dry at room temperature at least overnight. Slides were then deparaffinized to water in order to achieve optimal staining as follows: 3X5mins in xylene, 2X1 min in 100% Ethanol. For CHAD staining, heat induced epitope retrieval (HIER) method was not used. For Sox9, HIER was performed at pH=6,

and a temperature= 110°C for 5 minutes. For Cyr61, HIER was performed at pH=6, temperature=100°C for 10 minutes. Different HIER methods were required because antibody-antigen binding varied under different conditions for each antibody. A balance was struck between tissue preservation and antigen exposure. Once these steps were completed, slides were washed in cold running tap water X5 mins then rinsed in Tris-buffered saline (TBS) for 5 mins.

Many human tissues, including knee capsule contain endogenous peroxidases. In order to prevent false-positive staining in a peroxidase-dependent system (our DAB stain), we removed endogenous peroxidase activity using Peroxidazed 1 for 10 minutes (using dropper built into bottle to cover sample - 2-3 drops). Samples were rinsed X2 in TBS for 5 mins. Non-specific antibody binding was blocked using Background Sniper for 20 mins at room temperature (using dropper to cover sample - 2-3 drops). Excess Sniper was decanted. The sections were incubated with primary antibody diluted appropriately using DaVinci buffer, a pH=7.3 diluent with protein carrier and preservative used to improve necessary titers and reduce false-positive antibody binding. Antibody dilutions were as follows: CHAD 1:300; Sox9 1:125; Cyr61 1:20. The dilutions for CHAD and Cyr61 were as recommended by the manufacturer. The Sox9 titer was optimized in our lab from the manufacturers recommendation of 1:500. Incubations were done overnight at room temperature. Samples were then rinsed with TBS 2 X 5 minutes then incubated with Mach3 Rabbit HRP Polymere at room temperature for 10 minutes (using dropper to cover sample, about 2-3 drops). Samples were rinsed 2X in TBS for 5 minutes.

Slides were developed with DAB chromogen for 5 minutes. The mixture of DAB kit ingredients was as follows: 2250 µL ddH_2O, 250 µL 10X buffer, 2 drops chromogen. Ingredients were mixed in a vortex, then 1 drop H_2O_2 was added and the contents were mixed again. The mixture was added to the slides for 5 minutes, then slides were washed in running water.

Hematoxylin counterstaining was then performed using Shandon Instant hematoxylin for 15-20 seconds then rinsing in running tap water. In order to increase contrast between DAB and cells, the hematoxylin was diluted to half of the recommended concentration. After this, slides were dipped in the following solutions: Acid alcohol - 20 dips, Running tap water - rinse, ammonia water X1 min, running tap water 8 minutes.

Slides were then dehydrated as follows: 4 dips each of, 50% Ethanol, then 70% Ethanol, 100% Ethanol, and 100% Ethanol. Slides were then dipped in xylene dip X3, 4 dips each, then permount glue was added, 2-3 drops at edge of slide and slides were cover slipped and allowed to dry on a rack for 2 hours or overnight.

Immunohistology Microscopy and Data Analysis

IHC was used to confirm that protein production corresponded to the increase in expression of the 3 transcripts of interest (CHAD, Sox9, Cyr61). Samples were examined using the light microscope. Visualization was first performed at 2.5X magnification to appreciate the different types of tissues that were present in the sample. Four regions of each slide containing intact tissue were then examined at 50X magnification, avoiding the tissue periphery where substrate pooling and insufficient washings may give false positive staining. Regions were selected based on the overall composition of the tissue sample. For example, if the sample was 50% adipose and 50% fibrous, 2 regions showing adipose and 2 showing fibrous tissue were examined. In some regions selected, there were either no cells present or no cells were staining. We therefore decided to also examine the percentage of cells that were staining, including only those fields that showed cellular staining. Digital photos of each region were taken as described in the Histology section. Tissue was characterized by positive DAB (brown pigment) staining: nuclear, cytoplasmic, extracellular, types of cells that were stained, number of cells that stained and intensity of staining (0 = no staining, 1 = mild staining, 2 = moderate staining, 3 = intense staining). ImageJ was used to count the number of stained and unstained cells. This was done by opening the digital image in ImageJ, selecting "Plugins", then "Analyze", then "Cell counter". Cells were counted manually. The data from the cell counter window was input into Microsoft Excel 2010 and calculations were performed using this program. The percentage of cells that stained, the percentage of cells that stained including only fields showing staining cells, and the intensity of staining was compared between the 2 groups (contracture and no contracture). Statistical testing was performed using SPSS 16.0. The SPSS two-tailed T-test for independent samples analysis was used to obtain mean values. Statistical differences between groups were tested using the Mann-Whitney U test for non-parametric data. Parameters were considered statistically significantly different for p-

values < 0.05. Primary outcome measure was the percentage of cells staining in regions where cell staining was present. Secondary outcome measures included staining intensity and the percentage of cells staining including all fields. Finally, subcellular staining patterns were examined at 250X magnification using an oil-immersion lens.

Correlations between percent staining in areas of staining and staining intensity were calculated by comparing these data to the degree of flexion contracture. Correlations were calculated using SPSS 16.0. Both the Pearson (for parametric data) and Spearman (for non-parametric data) analyses were included.

Results

Subject Demographics and Associated Factors

Twenty subjects were recruited and their demographics recorded (see Tables 1 and 2). There was limited data in the literature on which to draw to determine which demographic data should be included. This was the first study looking at risk factors for contracture pre-operatively. A small number of TKA studies have looked at patient's characteristics which are risk factors for development of post-operative contracture and we included these in our study [10,66,68,75]. These included age, height, weight, BMI, total knee ROM and OA severity. In addition, we included factors based on our clinical experience that could contribute to or be associated with contracture of the knee before surgery. These included duration of OA, extension limitation and ROM of the contralateral knee, varus/valgus deformity of the surgical knee, level of activity and sports participation, use of gait aid, and prior non-surgical treatment, both pharmacologic and non-pharmacologic.

Recruited subjects included 13 (65%) subjects with contractures, and 7 (35%) controls. No subjects were found to have hyperextension (extension beyond 0°). Mean limitation to full extension in the contracture group was 9.5° (95% confidence interval ±0.9°) and 1.1°(±0.4°) in the control group. Contracture of the knee joint for surgery was associated with a lack of extension in the contralateral knee (3.8±1.0° in the contracture group compared to 0.6±0.4° in the control group; p=0.011), and duration of OA (15.5±3.9 vs 4.6±1.3 years in contracture and control groups respectively; p=0.038). There was a trend towards larger mean BMI in the contracture group (30.1±1.2 vs 26.4±1.2 kg/m^2; p=0.052). There was no statistically significant difference between groups for age, gender, height, weight, radiographic severity, or varus/valgus deformity of the surgical knee. Statistical significance for all characteristics was tested using the Mann-Whitney U test for non-parametric data. Results are summarized in Table 1. In addition to the characteristics identified above, there was no statistically significant difference found between the 2 groups for use of immunosuppressants, level of activity, use of gait aids, sports participation, pharmacologic treatment, or other non-pharmacologic treatments such as physiotherapy (see Table 2).

Table 1 – Demographics and Associated Factors of Subjects Undergoing TKA surgery

Demographic/Factor (mean)	**Contracture Group (Standard error) n = 13**	**Control Group (Standard error) n = 7**	**P value**
Age (years)	70.7 (2.9)	67.6 (2.6)	0.500
Gender (% male)	53.8	42.9	NS
Weight (kg)	82.6 (2.9)	74.2 (4.6)	0.088
Height (m)	166.2 (3.6)	167.6 (3.3)	0.812
BMI (kg/m^2)	30.1 (1.2)	26.4 (1.2)	0.052
Duration OA (years)	15.5 (3.9)	4.6 (1.3)	0.038
Radiologic Severity (Kellgren & Lawrence scale)	3.8 (0.1)	3.7 (0.2)	0.718
Varus or Valgus Deformity of Surgical Knee (°)	8.8 (1.8)	5.3 (1.6)	0.270
Maximum Surgical Knee Flexion (degrees)	112.5 (3.6)	121.7 (3.4)	0.151
Maximum Surgical Knee Extension (degrees) *	9.5 (0.9)	1.1 (0.4)	$p < 0.001$
Maximum Contralateral Knee Flexion (degrees)	125.4 (5.2)	126.6 (8.7)	0.320
Maximum Contralateral Knee Extension (degrees)	3.8 (1.0)	0.6 (0.4)	0.011

Table 2 - Additional Demographics of Recruited Subjects

Category	Variable	Contracture (n=13)	Control (n=7)
Use of Immunosuppressant		0	0
Level of Activity	Active	9	5
	Sedentary	4	1
Gait Aids	None	5	1
	Cane	4	3
	Walker	3	0
	Wheelchair	0	0
	Brace	1	2
Sports participation	Yes	7	2
	No	6	4
Pharmacological treatment	None or Tylenol	5	3
	NSAIDs	7	4
	Opiates	1	0
	Gabapentin (see below)	1	0
Joint injection		9	4
Other treatment	Physiotherapy	4	4

* = $p < 0.05$ (no characteristics met this)

Subject Matching for Microarray

Six patients each were selected from the contracture and control groups for a total of 12, corresponding to the number of samples that could be analyzed on a single Illumina HT-12 microarray chip. Because of the small sample size, we selected a number of demographics with which to match our patients (see methods). This differs from the usual method of selecting one or two factors on which to match, that would be preferable in larger sample sizes in order to minimize introduction of bias [76]. Demographic factors for the patients selected for microarray are listed in Table 3. There was a statistically significant difference for limitation of extension of the surgical knee. This was expected since the groups were segregated based on the presence of flexion contracture, which by definition is a limitation of extension. There was also a statistically significant difference in the amount of varus or valgus deformity of the contralateral knee.

In addition to patient-related factors, the selection of the 12 subjects was based on the matching quality of the total RNA extracted from sample tissues. Those with the highest quality were selected. Quality of RNA was determined using the RNA quality index (RQI, see material and methods for full description of RQI).

Table 3 - Demographics and Associated Factors of Patients for Microarray

	Contracture Mean (n=6)	Non-Contracture Mean (n=6)	p value
Amount of Extension Limitation of Surgical knee (degrees)	11.3	1.0	0.003
Duration OA (years)	7.0	9.1	0.624
Amount of Extension Limitation of Contralateral knee (degrees)	5.7	1.0	0.076
BMI (kg/m^2)	31.0	28.1	0.173
Severity OA (Kellgren & Lawrence Grade)	3.3	3.3	1.00
Varus/Valgus Deformity of Surgical Knee (°)	9.7 (3.1)	6.7 (1.7)	0.589
Varus/Valgus Deformity of Contralateral Knee (°)	7.8 (2.2)	2.7 (0.9)	0.029
Number of Subjects with Intercondylar or Posterior Osteophytes	6	5	NS
Ethnicity	All Caucasian	All Caucasian	1.00
Gender (percent female)	83.3	66.7	0.532
Age (Years)	69.7	65.3	0.470
Percent Patients with History of Joint Injection	33.3	33.3	1.00

RNA Extraction and Quality

Total RNA extraction was performed on the posterior-lateral or posterior-medial knee capsule tissue of selected subjects and was obtained at the time of their surgery for TKA. DNase was not used during RNA isolation as the amounts of total RNA extracted from capsule tissues was low and DNAse treatment had a degradative effect on the small amounts of RNA could be extracted (Figure 1B). Figure 1 shows a large percentage drop in the area of the 18S and 28S RNA peaks when comparing DNase treatment to no DNase treatment (compare Figure 1B to 1A). The 18S and 28S RNA peaks were most prominent without the use of the Qiagen column or DNase but there were a significant amount of RNA degradation products, as shown on the left portion of the graph in Figure 1C. Because of the compromise between less RNA degradation and fewer RNA degradation products, the method of using the Qiagen column only was selected.

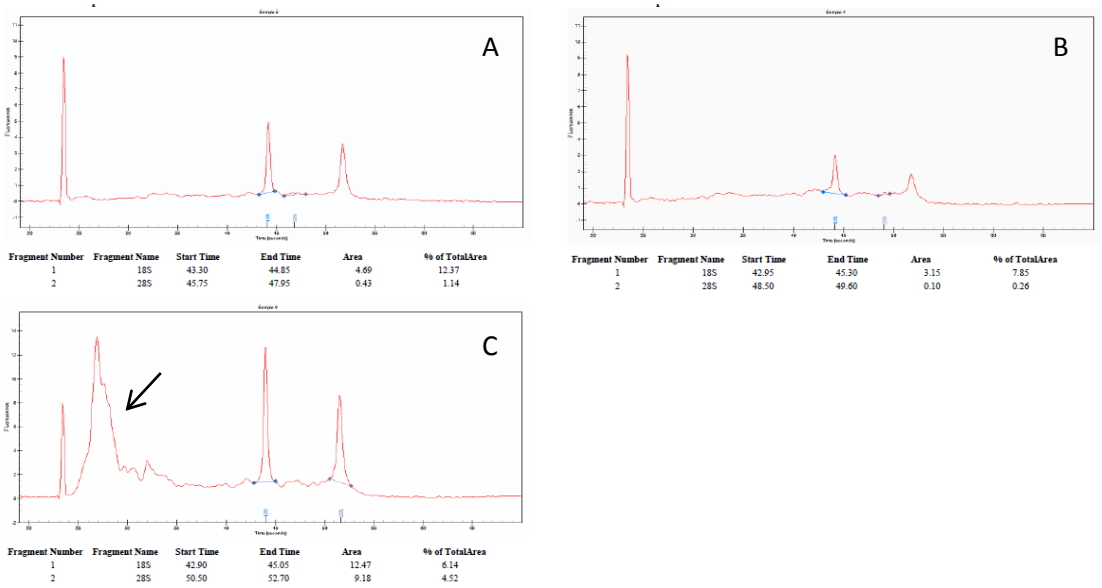

Figure 1 - Output from Experion StdSens RNA Analysis Software. Different methods used for RNA processing. A: Qiagen column only. B: Qiagen column and DNase. C: No Qiagen column or DNase. Note large peak of RNA degradation in C (arrow).

In order to ensure that there was no DNA contamination in the RNA samples used for microarrays, PCR reactions were performed using an RT-PCR protocol using either genomic DNA isolated from the blood of the subjects or their RNA as a template. Reactions were carried out using either RT-Taq polymerase (which can initiate PCR from a cRNA template generated by reverse transcriptase) or Taq polymerase (which cannot initiate the PCR reaction with RNA since it does not contain reverse transcriptase and therefore requires a DNA template). Figure 2 shows that there was no amplification of actin from the RNA samples tested using Taq polymerase (lanes 8 and 9), but there was good amplification of actin from the RNA samples using RT-Taq polymerase (lanes 6 and 7). As all other samples were treated with the same RNA isolation protocol, these results were extrapolated to the rest of the samples (i.e. no DNA present). Isolated total RNA for microarray was therefore cleaned with the Qiagen column only as described in the methods. Analysis of extracted RNA samples is summarized graphically in Figure 3 and numerically in Table 8. RNA samples had an RQI which ranged between 6.8 and 9.7, corresponding to medium to high quality. The lowest RQI in both groups was 6.8. The highest RQI in the non-contracture group was 9.2 and the mean RQI was 8.2, while the highest and mean RQI in the contracture group was 9.7 and 8.7 respectively. The differences in the means between the groups were not statistically significant ($p=0.172$ using the Mann-Whitney U test).

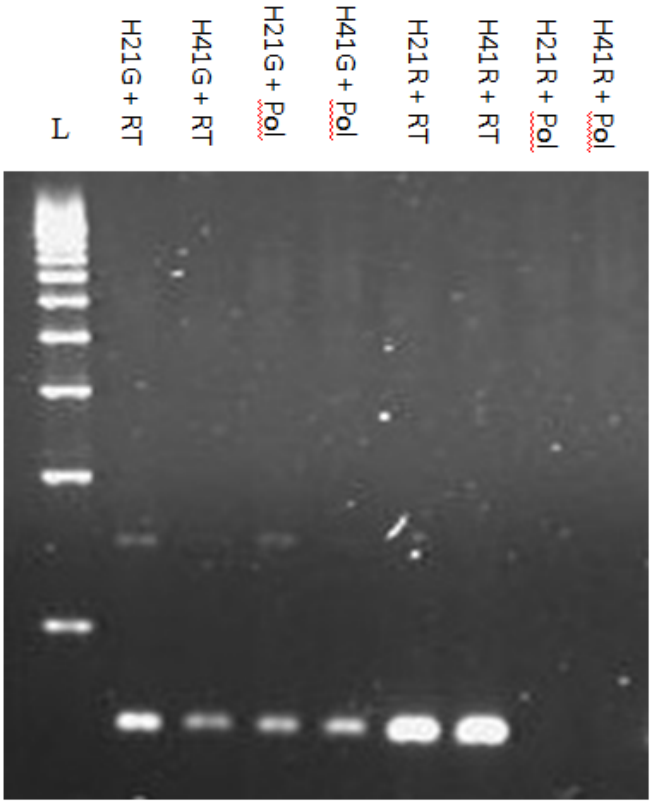

Figure 2. RT-PCR Reactions Using Either RT-polymerase Mixture or Polymerase alone With RNA or DNA Template. H21G: genomic DNA from subject H21; H41G: genomic DNA from subject H41; H21R: RNA isolated from subject H21; H41R: RNA isolated from subject H41. RT: Taq polymerase with reverse transcriptase; Pol: Taq polymerase without reverse transcriptase. The PCR product is Actin.

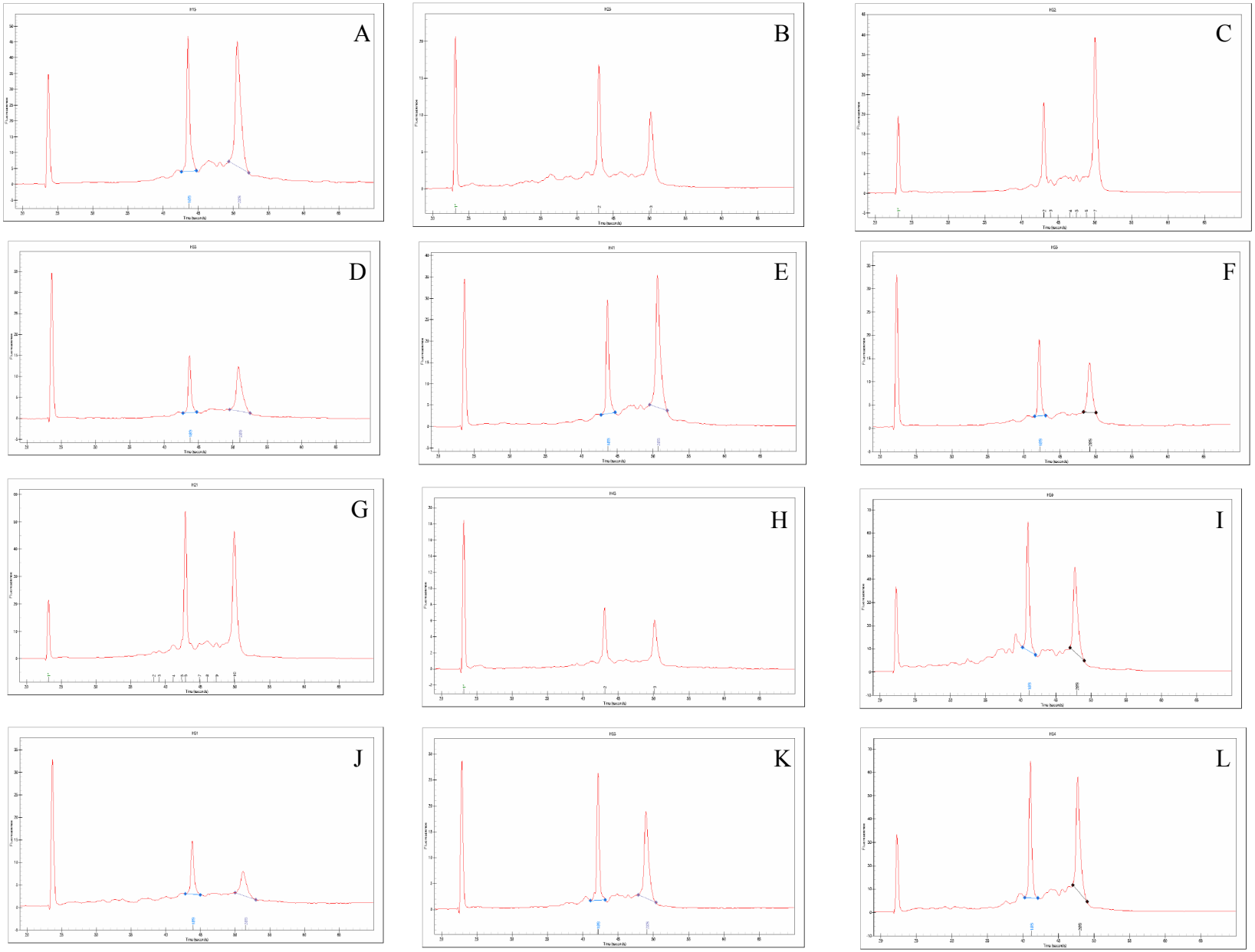

Figure 3. Experion StdSens Software Output for Extracted RNA Samples. Different panes correspond to different samples. A: H15, B: H25, C: H32, D: H33, E: H41, F: H55, G: H21, H: H43, H: H50, I: H51, J: H53, K: H54. Contractures are samples A-F, non-contractures are samples G-L.

Microarray Analysis

Microarray data analysis was carried out on 6 contracture patients and the 6 matched controls on RNA extracted from the posterior-medial or posterior-lateral knee capsule tissue (depending on which was available to the surgeon at the time of surgery). Statistical analysis of the gene expression was performed using various methods, as described in the materials and methods section to confirm that statistically significant genes remained significant with more than one statistical test (see Figure 4 for statistical strategy).

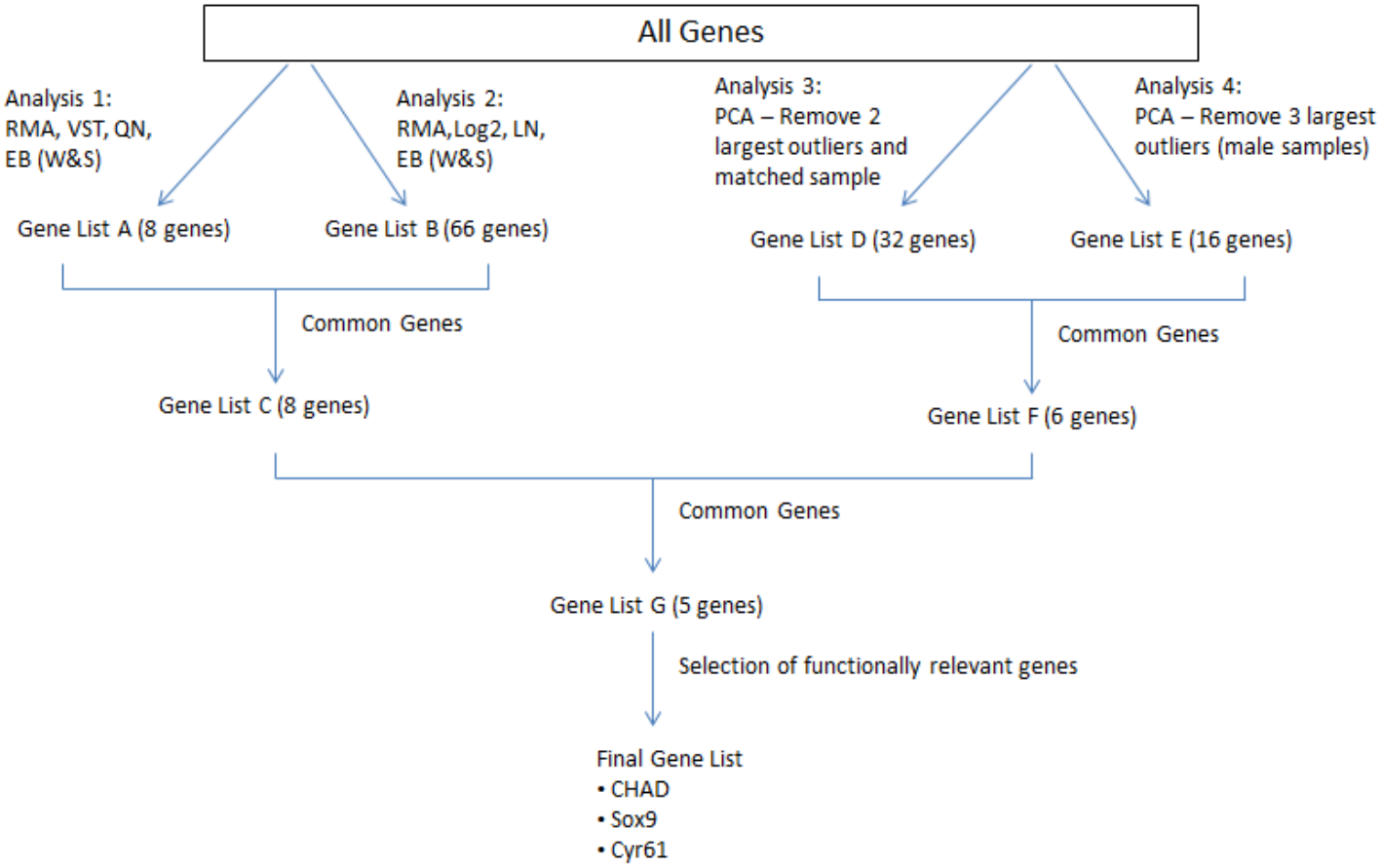

Figure 4. Statistical Analysis Strategy. RMA: Robust multiarray average, VST: Variance stabilization transformation, QN: Quantile normalization, EB: Empirical base, W&S: Wright and Simon. Analysis 3 and 4 also used RMA, VST, QN, EB (W&S).

Genes were considered statistically significant if they had a p value < 0.05 and a fold expression change greater than 2 or less than half when comparing contracture to control samples. Genes that were not expressed in any of the 12 samples analyzed were not removed for the statistical analyses. All false discovery analysis methods for multiple testing available in Flexarray, including Bonferroni, false discovery rate (2 methods), and family wise error rate (5 methods), eliminated all statistically significant genes. False discovery testing was therefore omitted from the analysis. Statistically significant gene transcripts discovered using RMA, variance-stabilizing transformation (VST), quantile normalization, and empirical base (Wright and Simon - EB W&S) including all samples in the analysis are shown in Table 4. Table 5 shows the analysis outcome including all samples using RMA, log2, Loess normalization, and W&S EB. Multivariate projection using Principle Component Analysis (PCA) was performed to determine if there were any subjects that were outliers in the major components of the microarray data. The first component outliers were the male subjects. Table 7 shows the significant genes with the males removed. Table 6 shows the significant genes with 2 of the males removed and their matched subjects. Genes in Tables 4 through 7 that are common between each analysis are highlighted in red and were considered for further analysis.

Five statistically significant genes were found based on $p < 0.05$ and fold expression greater than 2 or less than half. These genes included *Sox-9, CHAD, Cyr61, LOC649366*, and *casein alpha s1 (CSN1S1)*. LOC649366 is a predicted precursor of an isoform of aggrecan 1. When we investigated this gene further, we discovered that it had been removed from the NCBI Gene and Refseq databases and that there were no commercially available antibodies to it. We therefore decided to focus on other genes. *CSN1S1* is a gene whose product has a role in the capacity of milk to transport calcium phosphate and may play a role in immune modulation in milk [77]. Because of its only known role in milk, focus was placed on the other 3 genes. We therefore examined the expression of Sox9, CHAD, and Cyr61.

Table 4 - Microarray Results Using RMA, VST, Quantile Normalization and Wright and Simon Empirical Base With All Capsule Samples

Gene	Gene Definition (Provided by Flexarray)	log2(Fold change)	p-value
CCL19	Homo sapiens chemokine (C-C motif) ligand 19 (CCL19), mRNA.	-1.55	0.031
CHAD	Homo sapiens chondroadherin (CHAD), mRNA.	2.03	0.004
CILP	Homo sapiens cartilage intermediate layer protein, nucleotide pyrophosphohydrolase (CILP), mRNA.	1.35	0.040
CILP2	Homo sapiens cartilage intermediate layer protein 2 (CILP2), mRNA.	1.04	0.042
CSN1S1	Homo sapiens casein alpha s1 (CSN1S1), transcript variant 1, mRNA.	-2.80	0.040
CYR61	Homo sapiens cysteine-rich, angiogenic inducer, 61 (CYR61), mRNA.	1.41	0.002
LOC649366	PREDICTED: Homo sapiens similar to aggrecan 1 isoform 2 precursor (LOC649366), mRNA.	1.84	0.014
Sox9	Homo sapiens SRY (sex determining region Y)-box 9 (campomelic dysplasia, autosomal sex-reversal) (Sox9), mRNA.	1.14	0.007

Table 5 – Microarray Results Using RMA, Log2, Loess Normalization and Wright and Simon Empirical Base With All Capsule Samples

Gene	Gene Definition (Provided by Flexarray)	log2(Fold change)	p-value
ADORA2B	Adenosine A2b receptor (ADORA2B), mRNA.	-1.23	0.044
AOX1	Aldehyde oxidase 1 (AOX1), mRNA.	-1.46	0.040
BTC	Betacellulin (BTC), mRNA.	-1.65	0.003
C14ORF124	Chromosome 14 open reading frame 124 (C14orf124), mRNA.	1.02	0.029
C17ORF47	Chromosome 17 open reading frame 47 (C17orf47), mRNA.	1.37	0.047
CCL19	*Chemokine (C-C motif) ligand 19 (CCL19), mRNA.*	*-3.02*	*0.006*
CHAD	*Chondroadherin (CHAD), mRNA.*	*3.55*	*0.001*
CHST6	Carbohydrate (N-acetylglucosamine 6-O) sulfotransferase 6 (CHST6), mRNA.	2.06	0.045
CILP	*Cartilage intermediate layer protein, nucleotide pyrophosphohydrolase (CILP), mRNA.*	*1.32*	*0.024*
CILP2	*Cartilage intermediate layer protein 2 (CILP2), mRNA.*	*2.39*	*0.011*
CLDN11	Claudin 11 (oligodendrocyte transmembrane protein) (CLDN11), mRNA.	-1.39	0.019
CLIC5	Chloride intracellular channel 5 (CLIC5), mRNA.	-1.99	0.032
COL22A1	Collagen, type XXII, alpha 1 (COL22A1), mRNA.	-1.92	0.034
COL7A1	Collagen, type VII, alpha 1 (epidermolysis bullosa, dystrophic, dominant and recessive) (COL7A1), mRNA.	1.12	0.021
CSMD2	CUB and Sushi multiple domains 2 (CSMD2), mRNA.	1.46	0.010
CSN1S1	*Casein alpha s1 (CSN1S1), transcript variant 1, mRNA.*	*-3.35*	*0.024*
CYR61	*Cysteine-rich, angiogenic inducer, 61 (CYR61), mRNA.*	*1.47*	*0.001*
CYSLTR1	Cysteinyl leukotriene receptor 1 (CYSLTR1), mRNA.	-1.08	0.000
DLX5	Distal-less homeobox 5 (DLX5), mRNA.	1.08	0.004
DNASE1L3	Deoxyribonuclease I-like 3 (DNASE1L3), mRNA.	-1.66	0.049
ENPP4	Ectonucleotide pyrophosphatase/phosphodiesterase 4 (putative function) (ENPP4), mRNA.	-1.19	0.006

ERMP1	Endoplasmic reticulum metallopeptidase 1 (ERMP1), mRNA.	-1.06	0.003
FABP3	Fatty acid binding protein 3, muscle and heart (mammary-derived growth inhibitor) (FABP3), mRNA.	-1.50	0.026
FCGBP	Fc fragment of IgG binding protein (FCGBP), mRNA.	2.57	0.000
FMO3	Flavin containing monooxygenase 3 (FMO3), transcript variant 1, mRNA.	-1.39	0.049
GADD45G	Growth arrest and DNA-damage-inducible, gamma (GADD45G), mRNA.	1.24	0.020
GDF15	Growth differentiation factor 15 (GDF15), mRNA.	1.13	0.045
GDF5	Growth differentiation factor 5 (GDF5), mRNA.	-1.32	0.029
GEM	GTP binding protein overexpressed in skeletal muscle (GEM), transcript variant 1, mRNA.	1.05	0.040
GFRA3	GDNF family receptor alpha 3 (GFRA3), mRNA.	-1.40	0.029
GLB1L	Galactosidase, beta 1-like (GLB1L), mRNA.	-1.04	0.011
GPC4	Glypican 4 (GPC4), mRNA.	1.39	0.038
HAPLN1	Hyaluronan and proteoglycan link protein 1 (HAPLN1), mRNA.	1.87	0.034
HECW2	HECT, C2 and WW domain containing E3 ubiquitin protein ligase 2 (HECW2), mRNA.	-1.07	0.018
HIGD1B	HIG1 hypoxia inducible domain family, member 1B (HIGD1B), mRNA.	-1.15	0.007
HOXD10	Homeobox D10 (HOXD10), mRNA.	1.43	0.012
HS.344872	Clone IMAGE:1257951, mRNA sequence	1.53	0.023
HS.564389	DKFZp686C15231_r1 686 (synonym: hlcc3) cDNA clone DKFZp686C15231 5, mRNA sequence	-1.08	0.008
IFT74	Intraflagellar transport 74 homolog (Chlamydomonas) (IFT74), transcript variant 2, mRNA.	-1.01	0.007
KCNJ6	Potassium inwardly-rectifying channel, subfamily J, member 6 (KCNJ6), mRNA.	-1.70	0.012
KYNU	Homo sapiens kynureninase (L-kynurenine hydrolase) (KYNU), transcript variant 2, mRNA.	-1.25	0.046
LEFTY2	Left-right determination factor 2 (LEFTY2), mRNA.	1.77	0.002
LOC100134648	PREDICTED: similar to hCG2024106, transcript variant 2 (LOC100134648), mRNA.	1.29	0.046
LOC440993	Hypothetical gene supported by AK128346 (LOC440993), mRNA.	1.04	0.015
LOC649366	*PREDICTED: Similar to aggrecan 1 isoform 2 precursor (LOC649366), mRNA.*	*2.41*	*0.006*

LOC654433	Hypothetical LOC654433 (LOC654433), non-coding RNA.	1.31	0.012
LOC729254	PREDICTED: hCG2045843 (LOC729254), mRNA.	1.67	0.029
LOC730286	PREDICTED: misc_RNA (LOC730286), miscRNA.	1.06	0.041
LOXL4	Lysyl oxidase-like 4 (LOXL4), mRNA.	1.73	0.016
MFHAS1	Malignant fibrous histiocytoma amplified sequence 1 (MFHAS1), mRNA.	-1.54	0.001
MIA	Melanoma inhibitory activity (MIA), mRNA.	1.46	0.002
MKX	Mohawk homeobox (MKX), mRNA.	1.20	0.029
PHLDB2	Pleckstrin homology-like domain, family B, member 2 (PHLDB2), mRNA.	-1.22	0.001
PRRT2	Proline-rich transmembrane protein 2 (PRRT2), mRNA.	1.18	0.046
RNF150	Ring finger protein 150 (RNF150), mRNA.	-1.69	0.007
SELP	Selectin P (granule membrane protein 140kDa, antigen CD62) (SELP), mRNA.	-1.61	0.004
SEMA3A	Sema domain, immunoglobulin domain (Ig), short basic domain, secreted, (semaphorin) 3A (SEMA3A), mRNA.	-1.77	0.049
SOX15	SRY (sex determining region Y)-box 15 (SOX15), mRNA.	1.103156	0.044
SOX9	*SRY (sex determining region Y)-box 9 (campomelic dysplasia, autosomal sex-reversal) (SOX9), mRNA.*	*1.79*	*0.001*
TBC1D9	TBC1 domain family, member 9 (with GRAM domain) (TBC1D9), mRNA.	-1.03	0.004
THRA	Thyroid hormone receptor, alpha (erythroblastic leukemia viral (v-erb-a) oncogene homolog, avian) (THRA), transcript variant 2, mRNA.	1.01	0.036
TMEM176B	Transmembrane protein 176B (TMEM176B), mRNA.	-1.38	0.030
VIT	Vitrin (VIT), mRNA.	-1.22	0.034
XPNPEP2	X-prolyl aminopeptidase (aminopeptidase P) 2, membrane-bound (XPNPEP2), mRNA.	-1.55	0.013
ZKSCAN1	Zinc finger with KRAB and SCAN domains 1 (ZKSCAN1), mRNA.	-1.07	0.019
ZNF423	Zinc finger protein 423 (ZNF423), mRNA.	-1.24	0.016

Genes shaded in *Red* are common to Table 4 and Table 5.

Table 6 – Microarray Analysis: RMA, VST, Quantile Normalization – Removed Largest Outliers and Matched Capsule Samples

TargetID	log2(Fold change)	p-value
ANGPTL7	1.64	0.000
APOD	-1.01	0.001
ATF3	1.25	0.000
C2CD4B	1.11	0.002
CCL19	*-1.15*	*0.001*
CHAD	*1.93*	*0.000*
CHURC1	1.09	0.000
CILP	*1.05*	*0.000*
CILP2	1.13	0.007
CSN1S1	*-2.57*	*0.000*
CYR61	*1.61*	*0.000*
F5	-1.18	0.000
HBA1	-1.77	0.000
HBA2	-1.65	0.000
HBB	-1.42	0.001
HLA-DRB4	1.39	0.000
HLA-DRB6	1.00	0.000
LOC100134331	1.25	0.000
LOC647450	1.14	0.001
LOC649366	*1.66*	*0.000*
LOC652102	1.35	0.000
MT1X	1.07	0.000
MYOC	1.03	0.000

NLF2	1.26	0.000
PPP1R3C	1.08	0.000
RPS4Y1	-1.08	0.001
SCRG1	1.24	0.000
SERPINA1	1.07	0.002
SNHG5	1.01	0.000
SOX9	*1.06*	*0.001*
TCEAL2	1.20	0.000
TNMD	1.11	0.000

Genes shaded in *Red* are common to Tables 4-7.

Table 7 – Microarray Analysis: RMA, VST, Quantile Normalization Removing Males

Target ID	log2(Fold change)	p-value
ACTG2	-2.10	0.044
ALDH1A3	-1.04	0.011
ANKRD37	1.02	0.007
CHAD	*2.24*	*0.017*
CSN1S1	*-3.63*	*0.024*
CYR61	*1.46*	*0.008*
DLX3	-1.01	0.027
DLX5	1.03	0.018
FCGBP	1.01	0.005
LEFTY2	1.00	0.020
LOC649366	*1.79*	*0.040*
MUSTN1	-1.21	0.025
PI16	-1.85	0.017
PPP1R3C	1.10	0.000
SOX9	*1.35*	*0.016*
THBS1	1.33	0.040

Genes shaded in *Red* are common to Tables 4-7.

Table 8 - Summary of RNA Quality

Experimental Group	Sample	RNA Concentration (ng/mcL)	28S/18S	RQI
Controls (n = 6)				
	H21	103.8	1.16	9.2
	H43	21.2	0.92	8.2
	H50	102.5	0.87	7.0
	H51	18.7	0.75	6.8
	H53	19.1	1.01	8.8
	H54	76.2	1.08	9.1
Contractures (n = 6)				
	H15	40.5	1.43	9.6
	H25	43.1	0.79	6.8
	H32	58.8	2.12	9.7
	H33	14.4	1.33	9.7
	H41	29.3	1.55	9.5
	H55	21.4	0.85	7.1*

* Used RIN instead of RQI and the Experion Stdsens analyser did not provide an RQI for this sample (reason unknown). The RIN was obtained from the Genome Québec analysis of the RNA.

Gene Expression and Severity of Contracture Correlation

The magnitude of the microarray gene expression after RMA, VST, and QN was compared to the degree of flexion contracture in our subjects to see if there was a correlation ("dose-dependence") between the two. When including all 12 subjects, there was a correlation for each of CHAD, Sox9, and Cyr61 (p=0.001, 0.010, 0.014 respectively – Pearson correlation). This was not surprising since all non-contracture had lower expression of each gene within similar magnitudes compared to the contracture group and improved the line of best fit for the data (data not shown). When only the contracture samples were included in the analysis however, there was no statistically significant correlation (p=0.222, 0.579, 0.914 for CHAD, Sox9, and Cyr61 respectively – Pearson correlation). We therefore could not confirm a direct correlation between the increased expression of a single gene and loss of extension in the contracture group.

Confirmation of Microarray Results

RT-PCR and product band quantitation were used to confirm increased expression of *Sox9, CHAD,* and *Cyr61* genes in the contracture group, as identified in the microarray experiments. Genes were considered to be expressed differentially if the average intensity of the bands was statistically significant between the 2 groups (contracture and no contracture). The results are shown in Figure 5 and summarized in Table 9. There was a statistically significant difference in the expression of *CHAD* (p=0.040) and a trend towards difference in expression of *Sox9* and *Cyr61* (both p=0.055) genes.

Table 9 - Summary of PCR Band Quantitation

Gene	Average Expression Non-Contracture Group Relative to Actin (Peak Area)	Average Expression Contracture Group Relative to Actin (Peak Area)	p-value
CHAD	1.20	7.39	0.040
Sox9	0.48	0.95	0.055
Cyr61	3.34	11.65	0.055

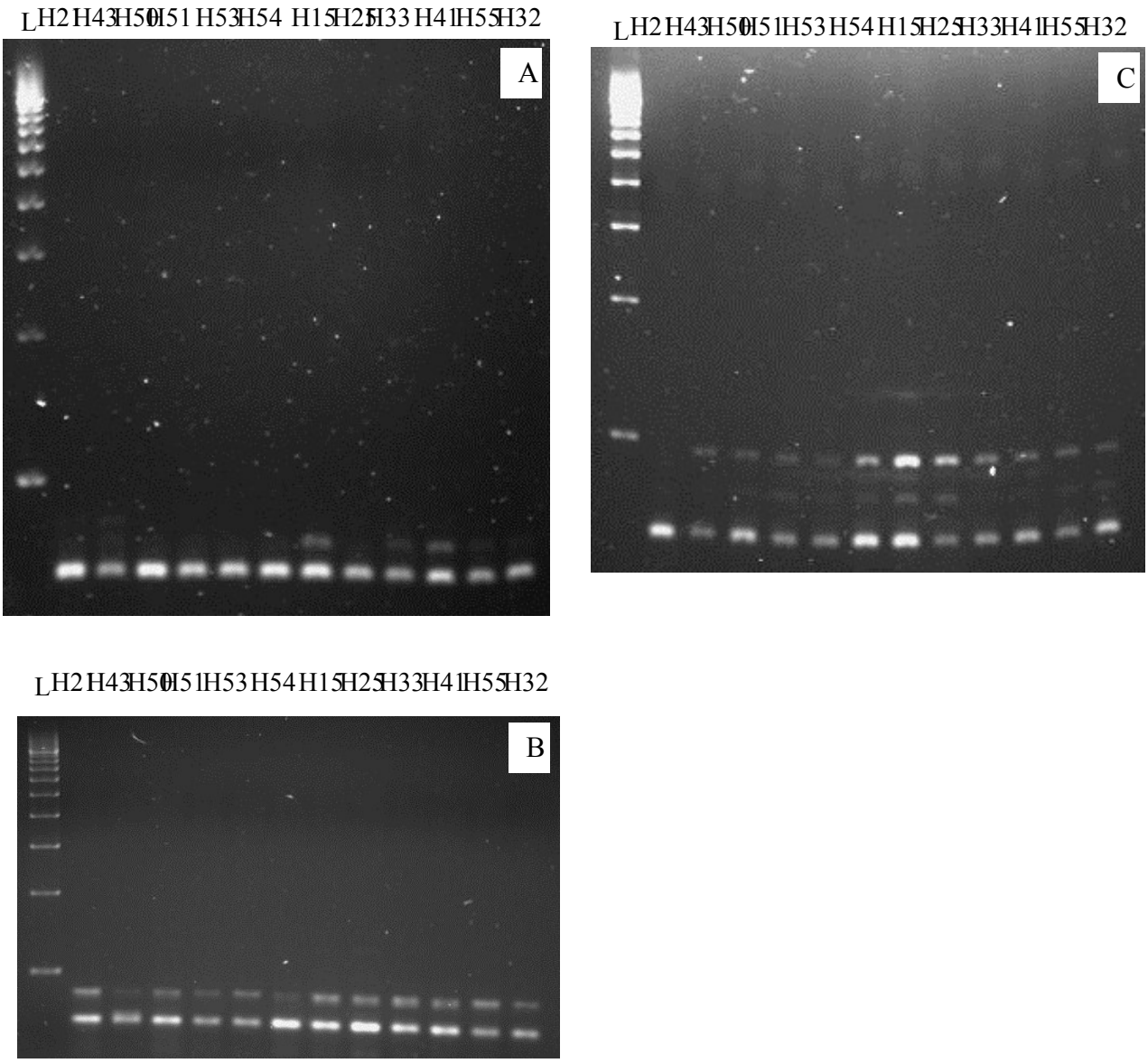

Figure 5. RT-PCR of Selected Genes. A: CHAD; B: Sox9; C: Cyr61. Labels at the top indicate sample number, L= 500 base ladder. Left-most 6 samples are non-contracture, right-most 6 samples are contracture. Major upper bands are gene of interest. Major lower bands are β-actin.

Histological Analysis

In order to better understand the cellular composition of the tissues on which we were performing microarray analysis, we characterized either posterolateral or posteromedial knee capsule tissue from the 12 patients whose tissue samples were used for microarray (6 with contracture and 6 without contracture). In addition, to our knowledge histological characterization comparing severe OA with contracture to severe OA without contracture has never been reported for capsular tissue from those patients. This provided us with a novel opportunity to study this important parameter.

Our knee capsule tissue was characterized based on the proportion of non-adipose, adipose, and synovial tissue. The average cross-sectional area of the entire tissue sample for the contracture group was 9.7 mm^2, and for the no contracture group 19.8 mm^2. We found a trend towards higher non-adipose, non-synovial cross-sectional area (87.0%, min:79.0%, max:100%), lower adipose (8.7%, min, max: 0%,19.1%) and lower synovial tissue (4.3%, min, max 0%,1.0%) in the contracture group compared with the group without contractures [69.1% (min, max: 25.4%,99.6%), 16.2% (min, max: 0%,45.1%), 14.7% (min, max: 0.4%,74.6%) respectively; p=0.731, 0.932, 0.521 respectively using Mann-Whitney U). The number of fibroblasts and adipocytes per high-powered field was similar between the two groups (contracture samples 23.6 and 14.3 respectively; non contracture 25.1 and 12.4 respectively). There was a large heterogeneity in the size and composition of the tissue samples in both groups. The results are summarized in Table 10.

Table 10 - Histological Characteristics of Contracture and No Contracture Groups

Histological Characteristic	Average of Severe OA with Contracture (min, max)	Average of Severe OA without Contracture (min,max)
Total Sample Area (mm^2)	9.7 (2.5, 21.2)	19.8 (3.3, 55.4)
% Adipose	8.7 (0, 19.1)	16.2 (0, 45.1)
% Non-adipose, Non-synovial	87.0 (79.0, 100)	69.1 (25.4, 99.6)
% Synovial Intima	4.3 (0, 21.0)	14.7 (0.4, 74.6)
Synovial Thickness (# Cells)	3.8 (0, 7)	4.9 (3, 6.5)
Avg. # Fibroblasts / HPF (Two 100X fields)	23.6 (4.5, 43)	25.1 (6, 73.5)
Avg. # Adipocytes / HPF (Two 50X fields)	14.3 (0, 31.5)	12.4 (0, 26)

Immunohistochemistry

We measured if the difference in mRNA expression we observed corresponded to a change in the amount of protein produced from the selected genes. We were able to adequately examine cellular and ECM staining in 4 regions for all samples. The results are summarized in Table 11.

Table 11 - Average Protein Expression of CHAD, Sox9 and Cyr61 Using Immunohistochemistry

	Types of Cells Present	Types of Cells Staining	Subcellular staining pattern	% Cells staining - all fields (min,max)	p-value	# fields showing staining	% Cells staining - only fields that show staining cells (min,max)	p-value	Average Staining Intensity	p-value
CHAD										
Non-contracture	Fibroblasts, Synoviocytes, Adipocytes, endothelial cells	Non-adipocytes	Nuclear Occasional pericellular ECM	14.5 (0,63.0)	NS	19	18.3 (1.1,63.0)	0.048	1.3	NS
Contracture	Fibroblasts, Synoviocytes, Adipocytes, endothelial cells	Non-adipocytes		26.0 (0,68.6)		18	34.6 (1.3,68.6)		1.4	
Sox9										
Non-contracture	Fibroblasts, Synoviocytes, Adipocytes, endothelial cells	Non-adipocytes	Nuclear and Cytoplasmic Little to no ECM	33.9 (0,100)	NS	20	40.7 (2.5,100)	NS	1.2	0.049
Contracture	Fibroblasts, Synoviocytes, Adipocytes, endothelial cells	Non-adipocytes		31.8 (0,100)		18	42.4 (0.9,100)		1.6	
Cyr61										
Non-contracture	Fibroblasts, Synoviocytes, Adipocytes, endothelial cells	Adipocytes (1 sample), non-adipocytes (all samples)	Nuclear and Cytoplasmic Little pericellular ECM	16.9 (0,71.8)	NS	18	22.5 (0.8,100)	NS	1.4	NS
Contracture	Fibroblasts, Synoviocytes, Adipocytes, endothelial cells	Adipocytes (2 samples), non-adipocytes (all samples)		17.0 (0,100)		20	20.4 (1.2,100)		1.4	

The parameters examined included the percentage of cells that were staining in the field selected and the intensity of the staining. Intensity was graded from 0 to 3 with 3 being the highest intensity (see materials and methods). In some regions selected, there were either no cells present or no cells were staining. We therefore decided to also examine the percentage of cells that were staining, including only those fields that showed cellular staining.

We found a statistically significant difference in the percentage of CHAD-stained cells in fields with stained cells ($p = 0.048$, Mann-Whitney U; see Table 11). There was no difference in the percentage of CHAD-stained cells when fields containing no stained cells were included. There was no difference in CHAD-staining intensity between contracture and no contracture samples ($p>0.05$). CHAD staining was mainly cellular, not cytoplasmic (Figure 6D), and with minimal ECM staining. Figure 5 shows representative samples for synovial, non-adipose, and adipose tissue. There was no staining of adipocytes in either group.

For Sox9, there was a statistically significant difference in staining intensity between the 2 groups ($p = 0.049$, Mann-Whitney U; see Table 11). There was no difference in the percentage of Sox-9 positive cells when comparing either all fields or only fields with staining. Sox-9 staining was localized to both the nucleus and the cytoplasm (Figure 7D), with rare staining of the ECM. Figure 6 shows a representative staining pattern for non-adipose, adipose, and synovial tissue. There was no staining of adipocytes in either group.

For Cyr61, there was no statistically significant difference in the percentage of Cyr61-positive cells or the staining intensity between the 2 groups (see Table 11). Cyr61 staining was localized to both the nucleus and the cytoplasm (Figure 8D). There was little staining of the ECM. Figure 7 shows representative staining pattern for non-adipose, adipose, and synovial tissues. Of the 3 antibodies used (CHAD, Sox9, and Cyr61), only Cyr61 showed adipocyte staining, which was present in both contracture and no contracture OA groups (Figure 8B).

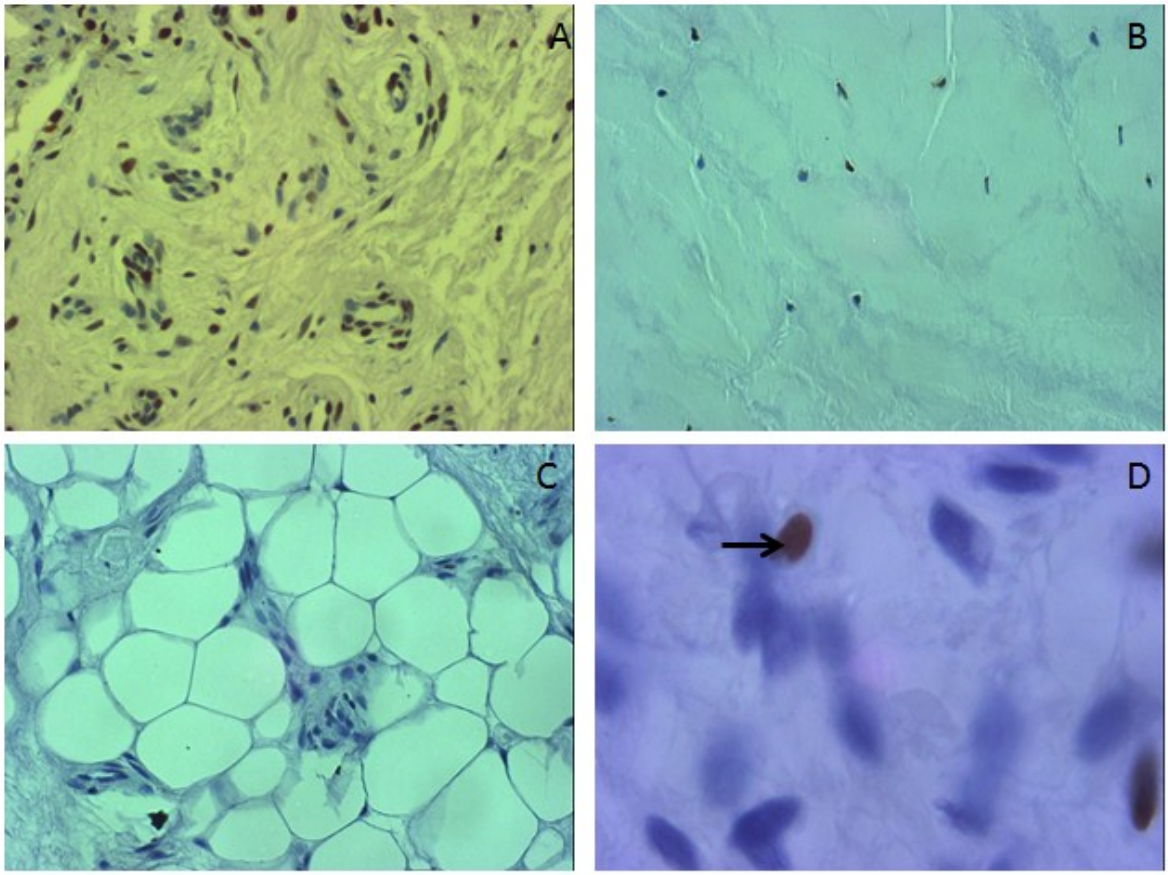

Figure 6. CHAD Immunohistochemistry of Posterior Knee Capsule. Light microscopy. A: 50X - Contracture sample showing proliferated synovium. B: 50X - Non-contracture showing fibrous tissue. C: 50X - Non-contracture showing adipose and fibrous tissue. D: Immunolocalization of CHAD to the nucleus (arrow) but not to the cytoplasm nor ECM - 200X. Counterstaining: hematoxylin.

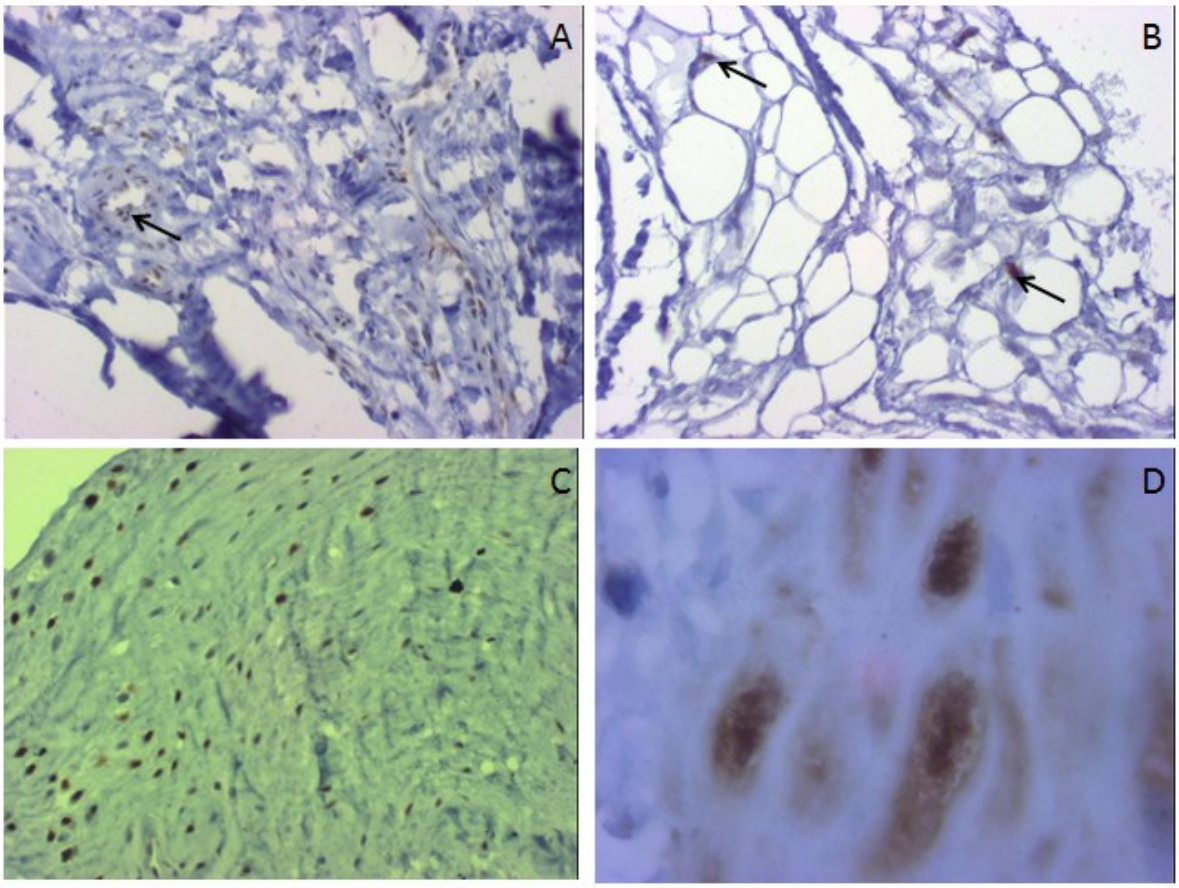

Figure 7. Sox9 Immunohistochemistry of Posterior Knee Capsule. Light microscopy. A: 50X – Non-contracture sample showing fibrous tissue and endothelial tissue (arrow). B: 50X - Contracture showing adipose tissue. Arrows: stained nuclei of supportive tissue cell. C: 50X - Contracture showing non-adipose tissue. D: Immunolocalization of Sox9 to the nucleus, cytoplasm, and ECM - 200X. Counterstaining: hematoxylin.

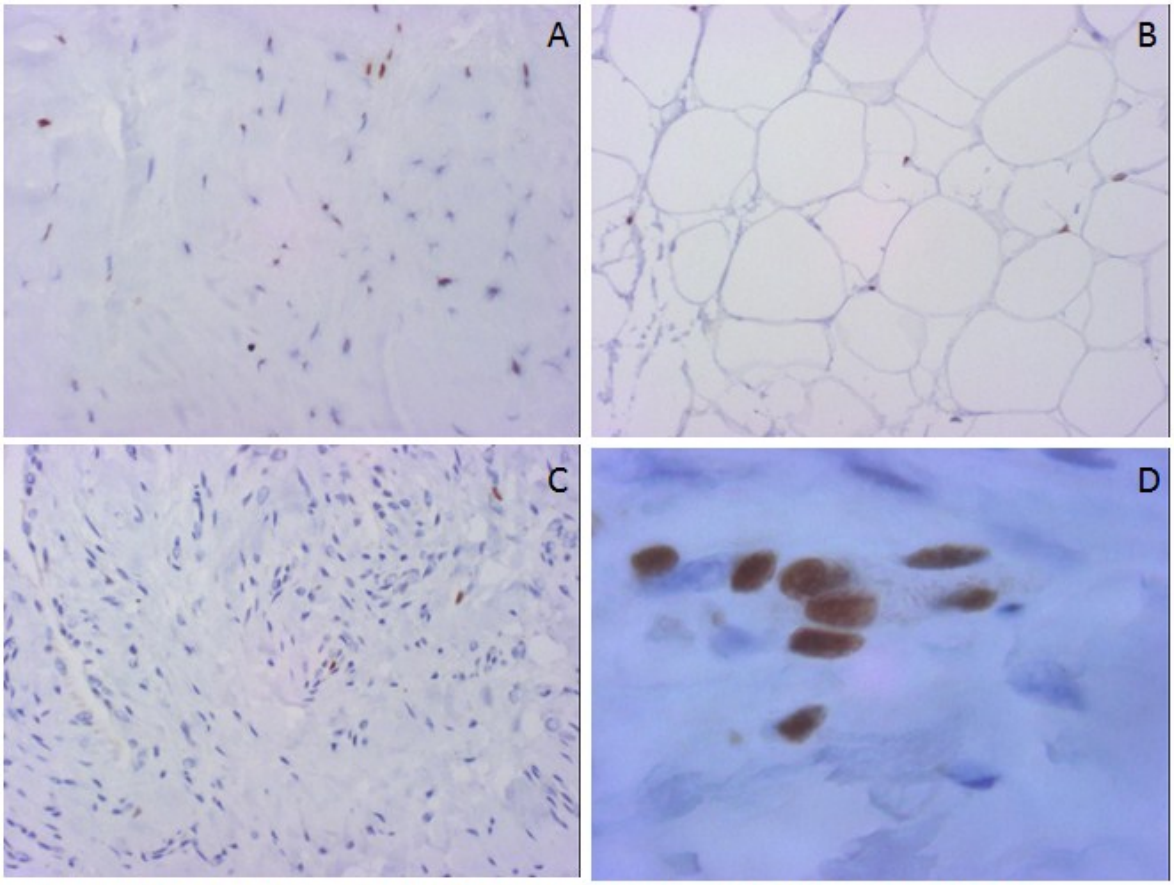

Figure 8. Cyr61 Immunohistochemistry of Posterior Knee Capsule. Light microscopy. A: 50X – Non-contracture sample showing fibrous tissue. B: 50X - Contracture showing adipose tissue. C: 50X - Contracture showing synovial and fibrous tissue. D: Immunolocalization of Cyr61 to the nucleus and cytoplasm – 200X. Counterstaining: hematoxylin.

Protein Production and Severity of Contracture Correlation

The percent staining in regions of staining and the staining intensity were compared to the severity of contracture to see if there was a correlation ("dose-dependence") between the two. There were no statistically significant correlations when including all 12 subjects, or only the contracture subjects (Pearson correlation).

Discussion

Knee flexion contracture decreases function and quality of life and predicts worse pain, function, and even contracture post-TKA [10,69]. In this study, we examined subjects with severe knee osteoarthritis requiring TKA. We determined patient factors that were associated with preoperative knee contracture. We found an association between duration of OA and loss of extension of the contralateral knee as well as a trend towards elevated BMI and knee flexion contracture. The posterior capsule has been shown to be an important contributor to a knee contracture; therefore, posterior knee capsule tissue was extracted intraoperatively. On these human capsules, we examined histologic features, gene expression patterns and protein products [15,30,61]. Histologically in the group with contracture, capsule tissue contained more fibrotic, less synovial and less fat tissue compared to the group without knee joint contracture, but not reaching statistical significance. We discovered increased expression of the genes *CHAD, Sox9*, and *Cyr61* in the contracture group along with correspondingly increased presence of the protein product for CHAD and Sox9.

The association between longer OA disease duration and knee joint contractures may be explained by mechanical causes. As knee cartilage degeneration progresses with OA, so does pain with weight-bearing in the extended position. In order to alleviate the pain, patients may hold their knee in a more flexed position, apposing cartilage surfaces with less degradation, thereby causing less pain from subchondral bone. Over time, never accessing the available range of extension would lead to structural changes of the soft tissues around the knee, including shortening of the posterior joint capsule. These changes would worsen with time, leading to increasing contracture severity with duration of OA.

Lack of extension in the contralateral knee may also be secondary to mechanical causes. Once one knee is severely affected by OA and develops a flexion contracture, it is functionally shorter [80]. There are a number of disadvantages to ambulating on legs of unequal length including altered center of pressure [81], pain in other joints [80], and increased energy requirements [82]. Patients may alter their gait to compensate for the leg length discrepancy. One way is to flex the contralateral knee. This reduces the effective

length of the intact leg during ambulation and restores equal leg length thereby correcting for some gait abnormalities and their consequences. The disadvantage is the potential loss in extension range in the contralateral knee, as we found in our study [80,81].

Another possible explanation for the higher prevalence of knee joint flexion contractures in the contralateral knee is a genetic predisposition. Supporting evidence comes from experiments using different rat strains subjected to the same environmental conditions and immobilization of the knee joint. In this model of immobility-induced contractures, Dark Agouti and Fisher 344 strains developed more severe contractures than Augustus Copenhagen Irish and Brown Norway strains [38]. These results suggested that intrinsic genetic factors participated in the process leading to joint contracture. In Sprague-Dawley rats, gene expression and protein levels in the capsule tissue were altered. Increased deposition of collagen I, but not collagen III may lead to fibrosis [15]. These changes only occur on the side of the joint not subjected to physiologic tension, that is, the posterior capsule [15,62]. Further experiments in a rat model have shown the expression of a number of other genes to be altered, including the inflammation-mediating COX-1 and COX-2 [39], chondrocyte-protecting Chitinase 3-like Protein 1 [40], anti-apoptotic protein Mcl-1 [41], and cartilage degeneration-mediating prothrombin [42]. Some patients with OA may display individual variation in the expression of genes or gene pathways contributing to contracture formation. Some individuals may therefore be genetically predisposed to developing joint contractures, increasing the risk of developing bilateral knee contractures. Evidence of genetic predisposition on capsular laxity has been described previously, though at the opposite end of the spectrum. Conditions such as Ehlers Danlos (due to various genetic deficiencies in collagen expression and synthesis) [83], and Marfan's syndrome (mutation in the fibrillin-1 gene) [84] affect joint range of motion by causing laxity in articular structures, mainly the capsule. Clearly gene expression can play an important role in joint ROM.

Whether mechanical or genetic, these results suggest that interventions to prevent leg length discrepancy may preserve range of motion in the contralateral leg. At present, it is not standard clinical practice to closely follow the range of motion of both knees in patients with OA, nor to measure their functional leg length. Knee flexion contractures are often first documented when the patient presents for surgical assessment. If contracture of

one knee is a risk factor for contracture of the contralateral knee, then treating leg length discrepancy prior to the development of bilateral contractures would be highly beneficial. Otherwise patients with a contracture in their non-OA knee prior to TKA will paradoxically present with a contracture post-TKA in their non-affected knee. A contracture in the non-OA knee, as we found in our study, may explain the increased risk for redeveloping a contracture in the TKA knee post-operatively, and the poorer outcome. If contractures are discovered pre-operatively, correcting the functional leg length discrepancy post-operatively could improve surgical outcome. Whether pre-op or post-op, correcting for leg length discrepancy can be done using shoe lifts. This would constitute a simple and inexpensive treatment with possible large Health Care System returns in terms of pain, disease prevention, OA prevention, and functional outcomes.

The association between elevated BMI and knee flexion contractures in OA patients can potentially be explained by a mechanical or a biological factor. Larger body weight increases load on the knee joints. This may accelerate cartilage degeneration over already degenerated cartilage. This would encourage patients to keep the knees flexed to appose less degenerated areas of cartilage, leading to contracture over time as described above. Biologically, increased expression of inflammatory markers such as cytokines and TNF-α are associated with obesity. Inflammation is a known trigger for fibrosis [85]. Persistent, chronic, low-grade inflammation in periarticular tissues of the joints may affect the range of motion by increasing the fibrous content of the joint capsule as suggested in our study. Controlling weight is a reversible factor that may therefore help prevent knee joint contracture in patients with severe OA.

In our study, 65% of patients had a flexion contracture of the OA knee before surgery, higher than the value of 35% in one large study [10]. The discrepancy may be explained by the small sample size of eligible patients we studied. A number of patients met exclusion criteria or full dataset were not available and they were excluded. There may also have been a selection bias. Misunderstanding between the investigators and some orthopedic surgeons led to early recruitment focused more on enrolling patients with contracture, and only later were controls equally included.

The joint capsule is composed of a number of different tissue types including fibrous (collagen and fibroblasts), adipose, synovium, blood vessels and nerves [78,79]. The synovium is located on the inner aspect of the joint lining the intra-articular space and is normally this is 2-4 cells thick [78]. The majority of the knee capsule is composed of fibrotic tissue, the precise composition of which is dynamic: the proportion of the different tissues making up the joint capsule depends on several factors, including developmental origins, direction of applied stress, and age [79]. There is no generally accepted "normal" proportion of each tissue in the knee capsule described in the literature that could be found despite an extensive search by the author.

In this first study on the composition of the joint capsule in OA patients with knee contracture, we divided tissues into adipose, synovium, and non-adipose, non-synovium (fibrous, vascular and neurologic). We referred to this latter component as "fibrotic" as the vast majority consisted of collagen and fibroblasts. We found that our contracture group had a higher proportion of fibrotic tissue. This is consistent with the animal models of knee immobilization [15]. Because our subjects were at the end-stage of their OA and had multiple factors which could contribute to contracture (e.g. presence of osteophytes, altered capsule), it was not possible to determine if the changes in the capsule were the primary source of contracture or secondary to another cause.

Reduced joint motion may lead to increased collagen deposition which further reduces joint motion, creating a positive feedback loop. In severe OA, there is ongoing chronic inflammation in the capsule [8,63,64]. Inflammation was linked to fibrotic tissue proliferation in a variety of conditions including normal wound healing, renal fibrosis associated with autoimmune disease, diabetic nephropathy and pulmonary fibrosis [86-90]. One major mediator of fibrosis is transforming growth factor-beta (TGF-β) which promotes collagen deposition via Smad-dependent transcription initiation of collagen I [87]. OA may be yet another condition in which chronic inflammation leads to capsule fibrosis over time, via the TGF-β or another pathway.

The contracture group in our study had a decreased proportion of synovial tissue. A contracture achieves relative immobilization and reduced use of the knee joint. This may reduce joint space inflammation by preventing contact between articular surfaces protected only by degenerated cartilage as the patient holds the joint in the most comfortable position

(the position where the healthiest cartilage bears weight). Injured chondrocytes release inflammatory mediators into the synovial fluid, thus exposing the synoviocytes to these mediators [63,64]. Reduced joint motion in contracture would create less apposition of degenerated articular cartilage and less cartilage injury resulting in reduced exposure of the synovium to inflammatory mediators. As the joint milieu is the likely cause for synovial proliferation, reduction in these inflammatory mediators could reduce this proliferation [160]. In this scenario, the cause of contracture is not increased inflammation, but pain-inhibited restriction of joint ROM leading to capsular shortening.

A decreased proportion of adipose tissue in the contracture group may be related to the increased proportion of fibrotic tissue, leaving less space available for adipose.

The data from our preliminary study show that the proportion of tissue types may be correlated with contracture development and/or severity. This may help generate prognostic tools for contracture in OA patients. Repeating this study with a larger sample size could produce statistically significant differences.

Microarray is routinely used to analyze gene expression in both the research and clinical setting [91]. Over 3000 studies have used microarray to identify genes involved in normal tissue function as well as human pathologic conditions [91]. DNA microarray helped determine prognosis in a number of disease states, including rheumatoid arthritis, B-cell lymphoma, central nervous system embryonic tumours, breast cancer and leukemia [92-96].

No prior study has looked for genes that are differentially expressed in patients with severe knee OA and contracture compared to severe knee OA without contracture. In this study we used microarray to examine differences in gene expression and to help generate hypotheses about the underlying mechanism of contracture formation. Using this method, we discovered 5 genes that differed in expression between the groups. We used several parallel statistical analyses to confirm that the differential expression of these genes was not secondary to limitations of one particular statistical method.

Microarray data have low intra-individual variation at varying time points, but high inter-individual variation [157]. In addition to pathologic states, a number of factors have been identified that influence gene expression between individuals [97,98,157]. Gender and

age are major factors contributing to genetic variability in microarray data [97,98,157]. Gender is often the most important contributor to this variability [97]. Using principle component analysis, we discovered that the most significant component separating our 2 groups was gender. This was the only identifiable component. Age was not found to be one of the 3 components of variability; however this may be due to our small sample size. BMI has also been found to contribute to inter-individual variation [157]; however this was not the case for our data.

We found that between 92 and 97 percent of genes were expressed at a level close to zero (looking at the lowest bin of the gene expression histogram, data not shown), also in keeping with prior studies showing that approximately 90% of genes are not expressed in many cell types [99]. Our results are biologically relevant as they are consistent with the primary known contributor of genetic variability (gender), and the proportion of genes expressed (less than 10%). Of the 5 genes showing differential expression, we selected 3 to study further as one was highly unlikely to be involved in contracture formation and the second was a predicted precursor whose gene identity was removed from the National Center for Biotechnology Information (NCBI) Gene and RefSeq [100].

Despite significant contribution to biomedical research and treatment, there are limitations to DNA microarrays. These include the array production (no 2 microarrays are exactly the same), RNA extraction methods, probe labelling techniques, lack of sensitivity for splice variants, and hybridization conditions [101,102]. Microarrays also require that the sequence of genes is known in order to detect them and has limited ability to distinguish between different gene isoforms [103]. Moreover, no standard universally accepted protocols for data analysis exist and different statistical methods can yield different results [91]. Because of these limitations, results of microarray experiments are often confirmed using methods such as RT-PCR and IHC, as we did in our study [91]. A number of studies have found a strong correlation between microarray and RT-PCR data, indicating that changes in gene expression seen on microarray are valid [104-107]. This is often not the case with IHC, however as changes in gene expression using both microarray and qRT-PCR have shown poor correlation with protein production [104,108-111]. Such poor correlation has been attributed to mRNA stability and decay, cellular translation regulation, and mechanisms of protein degradation, all of which can affect protein levels [108,110].

The semi-quantitative examination of protein production using IHC likely contributes to the difficulty of correlating RT-PCR (which is quantitative) with IHC [104]. Best clinical applicability is when mRNA and protein levels agreed with one-another [112].

In our study, the tissue directly adjacent to the histological section was processed for RNA extraction and microarray. In this fashion, the observed gene expression approximated as closely as possible the histologic tissue composition. Similarly, IHC determined if the change in gene expression resulted in changes in protein production in our samples. IHC allowed us to directly visualize which cell types were producing the proteins of interest. In this study, we showed agreement between mRNA expression and protein production in 2 of our 3 genes of interest. Three quarters of the 12 subjects included in the microarray (9 of 12) were female. It is therefore possible that our microarray and IHC results (discussed below), can only be applied to females with severe OA.

Our microarray results showed that CHAD expression was increased 4-fold in the contracture group (Table 4 – log2 change = 2.03). IHC localized CHAD to fibroblasts and synoviocytes but not adipocytes. CHAD staining was largely nuclear with occasional staining in the pericellular ECM (Figure 6). CHAD is a member of the small leucine-rich repeat proteoglycan (SLRP) family. The core protein of SLRPs contains 8-11 leucine-rich repeats (LRR) flanked by conserved cysteine residues [113]. The LRR is a structural motif that allows the molecule to adopt a horseshoe-like configuration important for protein-protein interactions [113]. CHAD was initially discovered in bovine cartilage isolates by its ability to bind to chondrocytes [2]. In that study, CHAD also bound to fibroblasts [114], and triple-helical collagen [115]. CHAD binds chondrocytes through the extracellular domain of $\alpha 2\beta 1$ integrin [113]. Binding to CHAD helped chondrocytes to maintain their round cellular morphology [116] and induced intracellular signaling via ERK phosphorylation. In summary, CHAD interaction with chondrocytes appear to be important for cellular and ECM communication and homeostasis.

Since its discovery, CHAD RNA and protein have been found in a number of tissues outside of cartilage including cornea, ciliary body, lens, retina, peripheral nerves, Purkinje cells of the cerebellum, enteroendocrine cells, pancreatic islet cells, and ovary [113]. This indicates roles outside of cartilage homeostasis that have not yet been fully

elucidated. Studies examining other members of the SLRP family, including biglycan, decorin, and fibromodulin have shown these proteins to be essential for fibrillogenesis and ECM organization [117]. Mice in which one or more of these SLRPs were knocked out developed various phenotypes consistent with collagen-deficit disorders including skin laxity and frailty (Ehlers-Danlos), abnormal bone collagen matrix (osteogenesis imperfecta), and corneal diseases [117]. These phenotypes are all secondary to defects in collagen type I fibrils which are loosely spaced and disorganized in orientation [117]. Type I collagen is the major type making up the joint capsule, accounting for over 80% of the collagen present, the remainder being type III [118]. An increase in expression of SLRPs has also been associated with increased fibrosis [88]. Decorin, biglycan, lumican and fibromodulin were all increased in patients with diabetic fibrotic nephropathy characterized by deposition of type I collagen within the mesangial matrix [88]. What is not clear is the role that these proteins played in the fibrotic kidney, whether pro-fibrotic or anti-fibrotic. In support of a profibrotic role, increased expression of lumican has been found in pancreatic fibroblasts, acinar and islet cells during acute pancreatitis and may contribute to transient fibrosis [88]. SLRPs' role in fibrosis may be through an interaction with TGF-beta [90]. In pro-fibrotic models, it could not be deciphered whether the increased SLRP production was the cause of, or in response to the increased fibrosis [88,90]. In support of anti-fibrotic models, rats overexpressing decorin showed reduced fibrosis, proteinuria, and expression of TGF-β [88]. In summary, proteins of the same family as CHAD, the SLRPs, play an important role in extracellular matrix regulation and collagen expression and organization. The pro- or anti-fibrotic properties of individual members of the SLRP family remain to be determined. In our study, CHAD may contribute to the increased amount of fibrotic tissue in the posterior knee capsules of OA patients with knee flexion contracture. Determining the mechanism by which this occurs, either through regulation of TGF-β, or other mechanisms, needs to be defined. This may help directing therapies towards reducing or even preventing joint contractures.

Our microarray results showed that Sox9 expression was increased 2.2-fold in the contracture group (Table 4 – log2 change = 1.14). Sox9 is a member of the sex-determining region Y (SRY)-box (Sox) transcription factors [119] and is located on chromosome 17

[120]. The genes of this family contain a high mobility-group box (HMG) domain that contributes to DNA binding in the minor groove, DNA bending, interaction with other transcription factors, and nuclear import or export [119]. To date, twenty Sox genes have been identified in humans [121]. Our IHC localized Sox9 to fibroblasts and synoviocytes but not adipocytes. Sox9 staining was nuclear and cytoplasmic with little to no staining in the ECM (Figure 7). In chondrocytes, Sox9 binds as a homodimer to a pair of the consensus sequences of Col2a1, Col9a1, Col27a1, or Matrilin-1, activating their transcription [122,123]. It also directed the expression of collagen 11 and aggrecan [119,124,125]. During embryogenesis of the mouse, Sox9 is expressed in all chondroprogenitors and chondrocytes except hypertrophic chondrocytes. It is also expressed in the male gonad, otic vesicle, heart, kidney, pancreas, intestine, and neural crest [119]. In the chick, Sox9 plays a role in gut development by being expressed in the mesoderm of the pyloric sphincter and the intestine endoderm [126]. During human embryonic development, Sox9 is expressed in the developing skeleton, testes, pancreas, neural tube, and kidney [127]. It plays an essential role to initiate mesenchymal condensation (aggregates of mesenchymal cells that later differentiate into chondrocytes) and to maintain chondrogenic potential in early stages of chondrogenesis [119]. Sox9 expression is regulated by a number of factors, including TGF-β via Smad3, and bone morphogenic protein [128-130]. Heterozygous mutations of Sox9 in humans causes campomelic dysplasia, a disease characterized by bowing of the long bones, shortened limbs, distinctive facial features including the Pierre Robin syndrome, and genital ambiguity [131,132].

In addition to its role in embryogenesis, Sox9 has been linked to the pathogenesis of OA [55,133,134]. In OA cartilage, levels of Sox9 expression decline [55,133,134]. Transfection of OA chondrocytes in culture with a recombinant adeno-associated virus (rAAV) *SOX9* vector increased expression levels and elevated protein synthesis of both proteoglycans and type II collagen to wild type levels [55]. Overall, Sox9 conferred an anabolic, regenerative effect on cartilage matrix in this model of OA.

The joint capsule collagen composition is dynamic [79]. The majority of collagen within the joint capsule is type I and type III [15,79]. In regions of fibrocartilagenous attachment to bone the capsule contains type II collagen [79,135]. The amount of type II

collagen progressively accumulates with age, possibly affected by developmental origin and loading experience [79]. The increased expression of Sox9 may influence the composition of the joint capsule by altering the expression of collagen II and proteoglycans as well as tissue development and gene regulation. Sox9 may therefore be a key player in capsular remodelling under conditions such as, OA and contracture. Sox9 activity is influenced by a number of factors including TGF-β [128,129]. As with CHAD, this inflammation and fibrosis mediator may modulate Sox9 expression through a mechanism that has not been described previously.

Our microarray results showed that Cyr61 expression was increased 2.7-fold in the contracture group (Table 4 – log2 change = 1.41). In our study, Cyr61 IHC staining was nuclear and cytoplasmic with minimal staining in the ECM immediately adjacent to the cells (Figure 8). Cyr61 (CCN1) is a member of the CCN group of proteins which include connective tissue growth factor (CTGF, or CCN2), nephroblastoma overexpressed protein (Nov, or CCN3) and 3 other members [136]. The CCN proteins have four common domains: an insulin-like growth factor binding protein (IGFBP) domain, a Von Willebrand factor domain, a thrombospondin-homology domain, and a cysteine knot, heparin-binding domain [136-138]. The CCN family of proteins is involved in processes including mitosis, tissue repair, apoptosis, ECM production, angiogenesis, and fibrosis [136,139-143]. CCNs link the cells they regulate with the ECM by binding to cellular adhesion molecules [136,144-147]. Cyr61 binds to αVβ3, αIIβ3, αMβ2 integrins as well as heparin-sulfate-containing proteoglycans (HSPG) including syndecan 4 and perlecan [146-147]. CCNs use specific structural domains to bind to these adhesion molecules and exert their effects [136].

The best-studied CCN family member is CCN2. CCN2 plays a significant role in embryologic development of cartilage and bone, as well as being a strong promoter of fibrosis [136,148,149]. In fact, constitutively elevated CCN2 expression is a hallmark of fibrosis [136,148,149]. Overexpression of CCN2 led to a potent fibrotic response [136,150]. CCN2 is an essential co-factor for TGF-β, augmenting its fibrotic effect in mice. Co-injection of both CCN2 and TGF-β caused a sustained fibrotic response more potent than injection of TGF-β alone [151].

CCN1 (Cyr61), the next best studied member, has been involved in tissue and fracture repair, and in angiogenesis [136,142]. This gene contains a Smad-binding motif inducible by TGF-β [152], possibly indicating a pro-fibrotic role for Cyr61, similar to CCN2. Experiments with knock-in mice carrying mutations in the α6β1 integrin-HSPG binding sites (required to bind to fibroblasts), but not the αVβ3 integrin binding site (required for angiogenesis) of Cyr61 demonstrated the opposite. Using a wound healing model, Cyr61 drove fibroblasts into senescence, upregulated antifibrotic genes (MMP2, MMP3, MMP9), and down-regulated profibrotic genes (Col1a1 and TGF-β1) [85]. In this experiment, fibroblast senescence was dependent on the activation of ERK and p38 MAPK pathways which triggered $p16^{INK4A}$ [85]. In knock-in mice, senescence in fibroblasts was reduced and there was an increase in type I collagen and TGF-β expression and an increase in type I collagen deposition. As further anti-fibrotic evidence, wounds of knock-in mice treated with purified CCN1 protein showed enhanced expression of MMP's and reduced collagen and TGF-β expression as well as increased fibroblast senescence [85]. Cyr61 may therefore play an anti-fibrotic role in this wound healing model. The anti-fibrotic effects of Cyr61 may be organ specific, depending on the extracellular milieu.

In summary, like CHAD and Sox9, Cyr61 has multiple biological functions which we are only beginning to discover and describe. These functions appear to depend highly on the cellular adhesion molecules present in the ECM. Also like CHAD and Sox9, Cyr61 belongs to a family of proteins whose members govern an even larger number of cellular processes.

When considering CHAD and Cyr61 together, there is evidence in the literature that these two genes do not play a pro-fibrotic role, but instead inhibit fibrosis [88,139]. It may be that joint capsule cells are attempting to counteract the fibrosis of capsular shortening and prevent contracture in order to protect valuable joint ROM. We also discovered that the three proteins we studied influenced and/or were influenced by TGF-β and Sox9 and Cyr61 were influenced by the TGF-β associated Smad pathway [128,129,152]. Fibrosis may therefore be directed by more numerous mechanisms, making its regulation more complex than we are currently aware.

There are several potential applications of our genetic discoveries. Microarray results have been used for diagnosis and prognosis for various diseases [92-96]. As microarray technology becomes less costly, it may be possible to examine the gene expression of the posterior knee capsule in patients with OA. This could be achieved through an arthroscopic biopsy. In capsules expressing high levels of CHAD, Sox9, and Cyr61, ROM exercises and physiotherapy could be implemented as part of a preventive treatment strategy. For those who require TKA, capsular tissue could be sampled during surgery. Because of the potential for a rapid turnaround time of microarray results (less than one week), a post-operative treatment plan could be similarly designed based on the results. Other treatment applications include gene therapy and pharmacologic interventions targeting contracture development. Gene therapy and pharmacologic treatments for non-articular fibrosis have already been successful in non-human models [90,139]. Rats overexpressing decorin show reduced renal fibrosis following cDNA transfer into skeletal muscle [90], and in an even simpler experiment, topical Cyr61 reduced wound fibrosis in mice [139].

Future research is needed to address a number of questions generated from our results. The first question is the mechanism by which each of our genes contributes to capsule fibrosis. This may be complex as more than one mechanism may play a role. Confirming a pro- or anti- fibrotic role for CHAD, Sox9, and Cyr61 is crucial to understand contracture pathogenesis and would have important therapeutic implications. The second question is the relative importance of each of our genes in the development of contracture. Determining that one gene plays a more significant role than the other two or that the expression of a gene depends indirectly on another gene, would have therapeutic implications by focusing on the most potent target (best bang for your buck). A third question is whether the results from the capsular biopsies could also be found in other tissues that are more accessible. For example, if the expression of one or more of our 3 genes in the capsule parallels that in the blood, or synovial fluid, then this could provide a less invasive method of obtaining gene expression results that could be performed in the clinic setting. Finally, because of the small sample size used in this study, it is important to ask whether our results can be repeated in a larger sample size. Using a larger sample size

may also provide additional genes that are differentially expressed, and shed more light on the mechanisms of contracture development.

Conclusion:

In this study, we examined patient factors that were associated with knee joint contracture in the setting of severe OA. We discovered an associating between duration of OA and reduced ROM in the contralateral knee as well as a trend towards increased BMI in the contracture group. Posterior knee capsule histology showed increased fibrous tissue with reduced synovial and adipose tissues in the contracture group, but this was not statistically significant. Gene expression analysis using microarray of tissue adjacent to the histologic samples showed an increase in CHAD, Sox9, and Cyr61. Agarose gel band quantitation of RT-PCR reactions showed a statistically significant increase in CHAD and a trend towards an increase in Sox9 and Cyr61. Increased tissue protein levels were found for CHAD and Sox9, but not Cyr61 using IHC. Due to the female predominance in our study population, our results should be taken with caution when considering males with severe OA.

The results of this study suggest that simple treatment options, such as following joint ROM, initiating early ROM treatment, and correcting leg-length discrepancy both pre- and post-operatively could improve outcome in patients with OA. Our study also adds evidence towards the undesirable health consequences of elevated BMI including its impact on joint function and pain. Finally, we have provided the first data on the genetics of contracture in OA, two common, debilitating conditions. Further research into the underlying mechanisms of knee capsule fibrosis in OA is essential in order to identify pharmacologic and genetic treatment options to improve function and quality of life of patients with joint contracture and OA.

References

1) Dudek N. Trudel G. Essentials of Physical Medicine and Rehabilitation. 2006.
2) Tew M, Forster W. *JBJS (British)*. 69-B(3). 1987.
3) Scudderi GR. The stiff total knee arthroplasy – causality and solution. The Journal of Arthroplasty. 20(4):23-26. 2005.
4) Singer BJ, *et al*. Incidence of ankle contracture after moderate to severe acquired brain injury. Arch Phys Med Rehabil. 85:1465-9. 2004.
5) Buschbacher RM, Porter CD. Deconditioning, Conditioning, and the Benefits of exercise. In Braddom RL: Physical Medicine and Rehabilitation, 2nd Ed. W.B. Saunders. Pp.706-8. 2000.
6) Pritzker KPH. in Osteoarthritis. Oxford University Press, New York. pp.56-57. 1998.
7) Revell PA. Mayston V. Lalor P. Mapp P. Annals of the Rheumatic Diseases. 47(4):300-7. 1988.
8) Bullough PG. in Histology for Pathologists 3rd Ed. Lippincott Williams and Wilkins, Philadelphia PA. pp.113-120. 2007.
9) Norkin C, White D. Measurement of Joint Motion: A guide to goniometry, 3rd ed. F.A. Davis Company, Philadelphia PA. 2003. pp.221-240.
10) Ritter MA, Lutgring JD, *et al*. The Role of Flexion Contracture on Outcomes in Primary Total Knee Arthroplasty J Arthroplasty. 22(8):1092–6. 2007.
11) Steultjens MPM, *et al.* Rheumatology 2000;39:955-961.
12) Campbell J, Waters RL., Thomas L., Lombardi R., Mayer C. Physical Therapy. 64:715. 1984.
13) Perry J, Antonelli D, Ford W. JBJS. 57:7:961-967. 1975.
14) Potter PJ., Kirby RL., MacLeod DA. American Journal of Physical Medicine and Rehabilitation. 69(3):144-147. 1990.
15) Matsumo F, Trudel G, Uhthoff K. High Collagen type I and low collagen type III levels in knee joint contracture. Acta Orthop Scand. 73;3:335-343. 2002.
16) http://neuromuscular.wustl.edu/msys/contract.html#rigid. Accessed Nov. 23, 2011.
17) Taricco LD, Aoki SS. Rehabilitation of an adult patient with arthrogryposis multiplex congenita treated with an external fixator. *Am J Phys Med Rehabil*. May 2009;88(5):431-4.
18) Arthrogryposis: http://emedicine.medscape.com/article/941917-overview. Accessed July 1, 2011.
19) McDonald CM, Han JJ, Gregory TC. In: Braddom Physical Medicine and Rehabilitation 4th Ed. Elsevier Saunders. Philadelphia PA. 2011. pp. 1106-1110.
20) Lim LE, Campbell KP. The sarcoglycan complex in limb-girdle muscular dystrophy. Neurol 11:443452. 1998.
21) Collagen Type VI-Related Disorders: http://www.ncbi.nlm.nih.gov/books/NBK1503/ accessed July 1, 2011.
22) Molnar GE, Alexander MA. Pediatric Rehabilitation. Hanley and Belfus. Philadelphia PA. 1999.
23) Hildebrand KA, Zhang M, Hart DA. Clin Orth Rel Res. 439:228–234. 2005.
24) Hildebrand KA, Zhang M, Hart DA. Clin Orth Rel Res. 456:85–91. 2006.

25) Tomasek J, Rayan GM. Correlation of α-smooth muscle actin expression and contraction in Dupuytren's disease fibroblast. *J Hand Surg Am*. 20:450–455. 1995.
26) Tomasek JJ, Gabbiani G, Hinz B, Chaponnier C, Brown RA. Myofibroblasts and mechano-regulation of connective tissue remodelling. *Nat Rev Mol Cell Biol*. 3:349–363. 2002.
27) Ritter MA, Campbell ED. *J Arthroplasty*. 22(8):1092–6. 2007.
28) Tanzer M, Miller J. The Natural History of Flexion Contracture in Total Knee Arthroplasty - A Prospective Study. Clin Orth Rel Res. (248):129-34. 1989.
29) Trudel G, Uhthoff HK. Arch Phys Med Rehabil. 81:6-13. 2000.
30) Trudel G, Uhthoff HK, Brown M. Extent and Direction of Joint Motion Limitation After Prolonged Immobility: An Experimental Study in the Rat. Arch Phys Med Rehabil. 80:1542-1547. 1999.
31) Trudel G, Zhou J, Uhthoff HK. Four Weeks of Mobility After 8 Weeks of Immobility Fails to Restore Normal Motion. Clin Orthop Relat Res. 466:1239–1244. 2008.
32) Michelsson JE. Thickness of the rabbit knee during and after immobilization. IRCS Med Sci Connect Tissue Skin Bone Pathol Surg Transplant. 7:36. 1979.
33) Akeson WH, Woo SL, Amiel D, Doty DH. Rapid recovery from contractures in rabbit hindlimbs: a correlative biomechanical and biochemical study. Clin Orthop Relat Res. 122:359–365. 1977.
34) Finsterbush A, Friedman B. Reversibility of joint changes produced by immobilization in rabbits. Clin Orthop Relat Res. 111:290–298. 1975.
35) Hildebrand KA, Sutherland C, Zhang M. Rabbit knee model of post-traumatic joint contractures: the long-term natural history of motion loss and myofibroblasts. J Orthop Res. 22:313–320. 2004.
36) Usuba M, Akai M, Shirasaki BS, Miyakawa S. Experimental joint contracture correction with low torque: long duration repeated stretching. Clin Orthop Relat Res. 456:70–78. 2007.
37) Van Harreveld PD, Lillich JD, Kawcak CE, Gaughan EM, Mclaughlin RM, Debowes RM. Clinical evaluation of the effects of immobilization followed by remobilization and exercise on the metacarpophalangeal joint in horse. Am J Vet Res. 63:282–288. 2002.
38) Laneuville O, Zhou J, Uhthoff HK, TrudelG. Clin Orth Rel Res. 456:36–41. 2006.
39) Trudel G, Deslauniers N, Uhthoff H, Laneuville O. Journal of Rheum. 28;9:2066-2074. 2001.
40) Trudel G, Recklies A, Laneuville O. Clin Orth Rel Res. 456:92–97. 2006.
41) Trudel G, Uhthoff HK, Laneuville O. BBRC. 333:247–252 2005.
42) Trudel G., Uhthoff HK, Laneuville O. Journal of Rheumatology. 32;8:1547-1555. 2005.
43) Lane NE, Schnitzer TJ. In Cecil Internal Medicine 23rd Ed. Saunders Elsevier, Philadelphia, PA 19103. pp.1993-8. 2008.
44) Felson DT**.** The epidemiology of knee osteoarthritis: results from the Framingham Osteoarthritis Study. Seminars in Arthritis and Rheumatism. 20(3): Suppl 1, 42-50. 1990.
45) Felson DT. Osteoarthritis. In: Harrison's Principles of Internal Medicine. 17th ed. Access Medicine. Chapter 326. 2008. Accessed July 3, 2011.

46) Valdes AM, Spector TD. The genetic epidemiology of osteoarthritis. Current Opinion in Rheumatology. 22:139–143. 2010.
47) MacGregor AJ. *et al.* Arthr Rheum. 43;11:2410–2416. 2000.
48) Loughlin J. Osteoarthritis and Cartilage. 19:342-345. 2011.
49) Meulenbelt I, Min JL, Bos S, et al. Identification of DIO2 as a new susceptibility locus for symptomatic osteoarthritis. Hum Mol Genet. 17:1867–1875. 2008.
50) Valdes AM, *et al.* Annals of the Rheumatic Diseases. 70;5:873-5. 2011.
51) Fahmi H, Martel-Pelletier J, Pelletier J, Kapoor M. Mod Rheumatol. 21:1–9. 2011.
52) Fahmi H, Pelletier JP, Mineau F, Martel-Pelletier J. 15d-PGJ(2) is acting as a 'dual agent' on the regulation of COX-2 expression in human osteoarthritic chondrocytes. Osteoarthritis Cartil. 10:845–8. 2002.
53) Fahmi H, Di Battista JA, Pelletier JP, Mineau F, Ranger P, Martel-Pelletier J. Peroxisome proliferator-activated receptor gamma activators inhibit interleukin-1beta-induced nitric oxide and matrix metalloproteinase 13 production in human chondrocytes. Arthritis Rheum. 44:595–607. 2001.
54) Boyault S, SimoninMA,Bianchi A, Compe E, LiagreB,Mainard D, et al. 15-Deoxy-delta12, 14-PGJ2, but not troglitazone, modulates IL-1beta effects in human chondrocytes by inhibiting NF-kappaB and AP-1 activation pathways. FEBS Lett. 2001;501:24–30.
55) Cucchiarini M, *et al.* Restoration of the Extracellular Matrix in Human Osteoarthritic Articular Cartilage by Overexpression of the Transcription Factor SOX9 Arthritis and Rheumatism. 56;1:158–167. 2007.
56) Karlsson C, *et al.* Genome-wide expression profiling reveals new candidate genes associated with osteoarthritis. Osteoarthritis and Cartilage 18: 581–592. 2010.
57) Zhu F, Wang P, Lee NH, Goldring MB, Konstantopoulos K. Prolonged Application of High Fluid Shear to Chondrocytes Recapitulates Gene Expression Profiles Associated with Osteoarthritis. PLoS ONE. 5(12):e15174. 2010.
58) Aigner T, Fundel K, Saas J, Gebhard PM, Haag J, Weiss T, *et al*. Large-scale gene expression profiling reveals major pathogenetic pathways of cartilage degeneration in osteoarthritis. Arthritis Rheum. 54:3533–44. 2006.
59) Fukui N, Miyamoto Y, Nakajima M, Ikeda Y, Hikita A, Furukawa H, et al. Zonal gene expression of chondrocytes in osteoarthritic cartilage. Arthritis Rheum. 58:3843–53. 2008.
60) Trudel G, Seki M, Uhthoff HK. J Rheumatol. 27(2):351-7. 2000A.
61) Trudel G, Uhthoff HK. Arch Phys Med Rehabil. 81:6-13. 2000.
62) Trudel G, Jabi M, Uhthoff HK. Arch Phys Med Rehabil. 84;1350. 2003.
63) Pritzker KPH. in Osteoarthritis. Oxford University Press, New York. pp.56-57. 1998.
64) Revell PA. Mayston V. Lalor P. Mapp P. Annals of the Rheumatic Diseases. 47(4):300-7. 1988.
65) Keeney JA, *et* al. Clin Orth Rel Res. 440:135–140. 2005.
66) Laskin RS, Burak B. *J Arthroplasty*. 22(4) Suppl. 1. 41-46. 2004.
67) Bellemans J, *et al*. *Clin Orth Rel Res*. 452. 78-82. 2006.
68) Anouchi YS. *Clin Orth Rel Res*. 331. 87-92. 1996.

69) Ritter MA, Harty LD, Davis KE, Meding JB, Berend ME. Predicting Range of Motion After Total Knee Arthroplasty. The Journal of Bone and Joint Surgery. 85-A (7): 1279-1285. 2003.
70) http://www.illumina.com/products/humanht_12_expression_beadchip_kits_v4.ilmn (accessed Dec.21, 2011).
71) http://www.cellular-products.com/Molecular-biochemical-reagent/Biochemical-reagent/DEPC/ (accessed Dec.7, 2011)
72) http://gqinnovationcenter.com/services/functionalGenomics/technoIlluminaExpression.aspx?l=e (accessed December 21, 2011).
73) Whole-Genome Gene Expression Direct Hybridization Assay Guide. Illumina Proprietary Catalog # BD-901-1002 Part # 11322355 Rev. A
74) Irizarry RA. Exploration, normalization, and summaries of high density oligonucleotide array probe level data. Biostatistics. 4(2):249-264. 2003.
75) Keeny JA. *Clin Orth Rel Res*. 440. 135-140. 2005.
76) Grobbee DE. Hoes AW. Clinical Epidemiology: Principles, Methods, and Applications for Clinical Research. Sudbury, Mass. : Jones and Bartlett Publishers. 2009.
77) Vordenbäumen S. *et al*. Casein a s1 Is Expressed by Human Monocytes and Upregulates the Production of GM-CSF via p38 MAPK. *J Immunol.* 186;592-601. 2011.
78) Young B, Lowe JS, Stevens A, Heath JW. Wheater's Functional Histology 4th Ed. WB Saunders Co. 2000.
79) Ralphs JR, Benjamin M. The joint capsule: structure, composition, ageing and disease. J. Anat. 184:503-509. 1994.
80) Friberg, O. Clinical Symptoms and Biomechanics of Lumbar Spine and Hip Joint in Leg Length Inequality. Spine. 8(6):643-651. 1983.
81) Mahar RK, Kirby RL, MacLeod DA. Simulated leg-length discrepancy: its effect on mean center-of-pressure position and postural sway. Arch Phys Med Rehabil. Dec;66(12):822-4. 1985.
82) Delacerda FG, Wikoff OD. Effect of Lower Extremity Asymmetry on Kinematics of Gait. Journal of Orthopaedic and Sports Physical Therapy. 3(3):105-107. 1982.
83) http://emedicine.medscape.com/article/1114004-overview#showall (accessed Jan.6, 2012).
84) Dietz HC, Cutting GR, Pyeritz RE, Maslen CL, Sakai LY, Corson GM, Puffenberger EG, Hamosh A, Nanthakumar EJ, Curristin SM, et al. Marfan syndrome caused by a recurrent de novo missense mutation in the fibrillin gene. Nature. 352:337e9. 1991.
85) Jun JL *et al*. The matricellular protein CCN1 induces fibroblast senescence and restricts fibrosis in cutaneous wound healing. Nature Cell Biology. 12(7):676-687. 2010.
86) Lukas JA, Hawkinkels C, Dijke PT. Exploring anti-TFG-beta therapies in cancer and fibrosis. Growth Factors. 29(4): 140–152. 2011.

87) Pohlers D, *et al.* TGF-β and Fibrosis in different organs - molecular pathway imprints. Biochimica et Biophysica Acta. 1792:746-756. 2009.
88) Schaefer L, *et al.* Small proteoglycans in human diabetic nephropathy: Discrepancy between glomerular expression and protein accumulation of decorin, biglycan, lumican, and fibromodulin. The FASEB Journal. 15:559-561. 2001.
89) Keane , M.P. , R.M. Strieter , and J.A. Belperio. Mechanisms and mediators of pulmonary fibrosis. *Crit. Rev. Immunol.* 25 : 429 – 463. 2005.
90) Isaka Y, *et al.* Gene therapy by skeletal muscle expression of decorin prevents fibrotic disease in the rat kidney. Nature Medicine. 2(4):418-423. 1996.

91) Auer H, Newson DL, Kornacker K. Expression Profiling Using Affymetrix GeneChip Microarrays. Methods Mol Biol. 509:35-46. 2009.
92) Devauchelle V. *et al.* DNA microarray allows molecular profiling of rheumatoid arthritis and identification of pathophysiological targets.Genes and Immunity. 5:597-608. 2004.
93) Shipp MA. e*t al.* Diffuse large B-cell lymphoma outcome prediction by gene expression profiling and supervised machine learning. Nature Medicine. 8(1):68-74. 2002.
94) Pomeroy SL.. *et al.* Prediction of central nervous system embryonal tumour outcome based on gene expression Nature. 415:436-442. 2002.
95) Cheang MCU. Gene Expression Profiling of Breast Cancer. Annu. Rev. Pathol. Mech. Dis. 3:67–97. 2008.
96) Yeoh EJ, Ross ME, Shurtleff SA, et al. Classification, subtype discovery, and prediction of outcome in pediatric acute lymphoblastic leukemia by gene expression profiling. Cancer Cell. 1(2):133-43. 2002.
97) Gohlmann H, Talloen W. Gene Expression Studies Using Affymetrix Microarrays. Chapman & Hall/CRC Press. 6000 Broken Sound Parkway NW. 2009.
98) Gagnon-Bartsch JA, Speed TP. Using control genes to correct for unwanted variation in microarray data. Biostatistics. Nov 17. 2011. (Epub ahead of print).

99) European bioinformatics Institute. http://www.ebi.ac.uk/microarray/biology_intro.html. (accessed Jan.22, 2012).
100) NCBI Technical Support. Personal Communication.
101) Jonsdottir K, Størkson R, Krog1 A, Bukholm IRK. Correlation between mRNA Detected by Microarrays and qRT-PCR and Protein Detected by Immunohistochemistry of Cyclins in Tumour Tissue from Colonic Adenocarcinomas. *The Open Pathology Journal. 2,* 96-101. 2008.
102) Shendure J. The beginning of the end for microarrays? Nature methods. 5(7):585-587. 2008.
103) Wang Zhong, Gerstein M, Snyder M. RNA-Seq: a revolutionary tool for transcriptomics. Nature Reviews Genetics. 10:57-63. 2009.
104) Jonsdottir K, Størkson R, Krog1 A, Bukholm IRK. Correlation between mRNA Detected by Microarrays and qRT-PCR and Protein Detected by Immunohistochemistry of Cyclins in Tumour Tissue from Colonic Adenocarcinomas. *The Open Pathology Journal. 2,* 96-101. 2008.

105) Dallas PB, Gottardo NG, Firth MJ, et al. Gene expression levels assessed by oligonucleotide microarray analysis and quantitative real-time RT-PCR -- how well do they correlate? BMC Genomics. 6: 59. 2005.
106) Lin YM, Furukawa Y, Tsunoda T, et al. Molecular diagnosis of colorectal tumors by expression profiles of 50 genes expressed differentially in adenomas and carcinomas. Oncogene. 21: 4120-8. 2002.
107) Morey JS, Ryan JC, Van Dolah FM. Microarray validation: factors influencing correlation between oligonucleotide microarrays and real-time PCR. Biol Proced Online. 8: 175-93. 2006.
108) Kendrick N. Kendrick Labs Inc. http://www.kendricklabs.com/WP1_mRNAvsProtein.pdf. Nov.21, 2011.
109) Tian, Q., et al., Integrated genomic and proteomic analyses of gene expression in Mammalian cells. Mol Cell Proteomics. 3(10):960-9. 2004.
110) Vogel C., *et al.* Sequence signatures and mRNA concentration can explain two-thirds of protein abundance variation in a human cell line. Mol Syst Biol. 6:400. 2010.
111) Lundberg E, *et al.* Defining the transcriptome and proteome in three functionally different human cell lines. Mol Syst Biol. 6:450. 2010.
112) Dickson, BC, *et al*. High level JAG1 mRNA and protein predict poor outcome in breast cancer. Mod Pathol. 20(6):685-93. 2007.
113) Tasheva ES, Ke A, Conrad GW. Analysis of the expression of chondroadherin in mouse ocular and non-ocular tissues *Molecular Vision.*10:544-554.2004
114) Sommarin Y, Larsson T, Heinegard D. Chondrocyte-Matrix Interactions - Attachment to Proteins Isolated from Cartilage. Experimental Cell Research 184:181-192. 1989.
115) Månsson, B., Wengle´n, C., Mo¨rgelin, M., Saxne, T., and Heinegård, D. *J. Biol. Chem.* 276, 32883–32888.2001.
116) Woods, A., Longley, R. L., Tumova, S., and Couchman, J. R. *Arch. Biochem. Biophys.* 374, 66–72. 2000.
117) Ameye L, Young MF. Mice deficient in small leucine-rich proteoglycans: novel *in vivo* models for osteoporosis, osteoarthritis, Ehlers-Danlos syndrome, muscular dystrophy, and corneal diseases. Glycobiology. 12(9):107R-116R. 2002.
118) Kleftogiannis F, Handley CJ, Campbell MA (1994). Characterization of extracellular matrix macromolecules from bovine synovial capsule. J Orthop Res 12:365-374.
119) Akiyama H. Control of Chondrogenesis by Transcription Factor Sox9. Mod Rheumatol. 18:213-219. 2008.
120) Tommerup *et al.* Assignment of an Autosomeal Sex Reversal Locus (SRA1) and Campomelic Dysplasia (CMPD1) to 17q24.3-q25.1. Nature Genetics. 4:170-174. 1993.
121) Tavella S, Biticchi R, Schito A, Minina E, Di Martino D, Pagano A, et al. Targeted expression of SHH affects chondrocyte differentiation, growth plate organization, and Sox9 expression. J Bone Miner Res.19(10):1678–88. 2004.

122) Bernard P, Tang P, Liu S, Dewing P, Harley VR, Vilain E. Dimerization of SOX9 is required for chondrogenesis, but not for sex determination. Hum Mol Genet. 12(14):1755–65. 2003.
123) Sock E, Pagon RA, Keymolen K, Lissens W, Wegner M, Scherer G. Loss of DNA-dependent dimerization of the transcription factor SOX9 as a cause for campomelic dysplasia. Hum Mol Genet. 12(12):1439–47. 2003.
124) Ng LJ, Wheatley S, Muscat GE, Conway-Campbell J, Bowles J, Wright E, et al. SOX9 binds DNA, activates transcription, and coexpresses with type II collagen during chondrogenesis in the mouse. Dev Biol. 183(1):108–21. 1997.
125) Zhao Q, Eberspaecher H, Lefebvre V, De Crombrugghe B. Parallel expression of Sox9 and Col2a1 in cells undergoing chondrogenesis. Dev Dyn. 209(4):377–86. 1997.
126) Theodosciou NA, Tabin CJ. Sox9 and Nkx2.5 determine the pyloric sphincter epithelium under the control of BMP signaling. Developmental Biology. 279:481-490. 2005.
127) Piper, K., Ball, S., Keeling, J., Mansoor, S., Wilson, D., Hanley, N. Novel SOX9 expression during human pancreas development Correlates to abnormalities in Campomelic dysplasia. Mech. Dev. 116 (1–2):223– 226. 2002.
128) Furumatsu T, Ozaki T, Asahara H. Smad3 activiates the Sox9-dependent transcription on chromatin. The International Journal of Biochemistry and Cell Biology. 41:1198-1204. 2009.
129) Furumatsu T, Tsuda M, Taniguchi N, Tajima Y, AsaharaH. Smad3 induces chondrogenesis through the activation of SOX9 via CREB-binding protein/p300 recruitment. J Biol Chem. 280:8350–843. 2005.
130) Theodosciou NA, Tabin CJ. Sox9 and Nkx2.5 determine the pyloric sphincter epithelium under the control of BMP signaling. Developmental Biology. 279:481-490. 2005.
131) Hunag w, Lu Ni, Eberspaecher H, de Crombrugghe. A New Long FOrm of c-Maf Cooperates with Sox9 to Activate the Type II Collagen Gene. The Journal of Biological Chemistry. 277(52):50668-50675. 2002.
132) http://ghr.nlm.nih.gov/condition/campomelic-dysplasia (accessed Dec.18, 2011).
133) Salminen H, Vuorio E, Saamanen AM. Expression of Sox9 and type IIA procollagen during attempted repair of articular cartilage damage in a transgenic mouse model of osteoarthritis. Arthritis Rheum 44:947–55. 2001.
134) Aigner T, Gebhard PM, Schmid E, Bau B, Harley V, Poschl E. SOX9 expression does not correlate with type II collagen expression in adult articular chondrocytes. Matrix Biol. 22:363–72. 2003.
135) Bosczczyk BM, *et al.* An Immunohistochemical Study of the Dorsal Capsule of the Lumbar and Thoracic Facet Joints. SPINE. 26(15):E338–E343. 2001.
136) Leask A, Abraham DJ. All in the CCN family: essential matricellular signaling modulators emerge from the bunker. Journal of Cell Science. 119:4803-4810. 2006.
137) Bork P. The modular architecture of a new family of growth regulators related to connective tissue growth factor. *FEBS Lett.* 327, 125-130. 1993.

138) Perbal B. CCN proteins: multifunctional signalling regulators. *Lancet* 363, 62-64. 2004.
139) Jun JL *et al*. The matricellular protein CCN1 induces fibroblast senescence and restricts fibrosis in cutaneous wound healing. Nature Cell Biology. 12(7):676-687. 2010.
140) Igarashi A, Okochi H, Bradham DM, Grotendorst GR. Regulation of connective tissue growth factor gene expression in human skin fibroblasts and during wound repair. *Mol. Biol. Cell* 4:637-645. 1993.
141) Latinkic BV, Mo FE, Greenspan JA, Copeland NG, Gilbert DJ, Jenkins NA, Ross, SR, Lau LF. Promoter function of the angiogenic inducer Cyr61gene in transgenic mice: tissue specificity, inducibility during wound healing, and role of the serum response element. *Endocrinology* 142:2549-2557. 2001.
142) Leu SJ, Lam SC, Lau LF. Pro-angiogenic activities of CYR61 (CCN1) mediated through integrins alphavbeta3 and alpha6beta1 in human umbilical vein endothelial cells. *J. Biol. Chem.* 277:46248-46255. 2002.
143) Inoki I, Shiomi T, Hashimoto G, Enomoto H, Nakamura H, Makino K, Ikeda E, Takata S, Kobayashi K, Okada Y. Connective tissue growth factor binds vascular endothelial growth factor (VEGF) and inhibits VEGF-induced angiogenesis. *FASEB J.* 16:219-221. 2002.
144) Ellis PD, Metcalfe JC, Hyvonen M, Kemp PR. Adhesion of endothelial cells to NOV is mediated by the integrins alphavbeta3 and alpha5beta1. *J. Vasc. Res.* 40:234-243. 2003.
145) Schober JM, Lau LF, Ugarova TP, Lam SC. Identification of a novel integrin alphaMbeta2 binding site in CCN1 (CYR61), a matricellular protein expressed in healing wounds and atherosclerotic lesions. *J. Biol. Chem*. 278:25808-25815. 2003.
146) Leu SJ, Liu Y, Chen N, Chen CC, Lam SC, Lau LF. Identification of a novel integrin alpha 6 beta 1 binding site in the angiogenic inducer CCN1 (CYR61). *J. Biol. Chem*. 278:33801-33808. 2003.
147) Leu SJ, Chen N, Chen CC, Todorovic V, Bai T, Juric V, Liu Y, Yan G, Lam SC Lau LF. Targeted mutagenesis of the angiogenic protein CCN1 (CYR61). Selective inactivation of integrin alpha6beta1-heparan sulfate proteoglycan coreceptor-mediated cellular functions. *J. Biol. Chem.* 279:44177-44187. 2004.
148) Blom IE, Goldschmeding R, Leask A. Gene regulation of connective tissue growth factor: new targets for antifibrotic therapy? *Matrix Biol.* 21:473-482. 2002.
149) Leask A, Abraham DJ. The role of connective tissue growth factor, a multifunctional matricellular protein, in fibroblast biology. *Biochem. Cell Biol*. 81:355-363. 2003.
150) Bonniaud P, Martin G, Margetts PJ, Ask K, Robertson J, Gauldie J, Kolb M. Connective tissue growth factor is crucial to inducing a profibrotic environment in "fibrosis-resistant" BALB/c mouse lungs. *Am. J. Respir. Cell Mol. Biol.* 31:510-516. 2004.
151) Mori T, Kawara S, Shinozaki M, Hayashi N, Kakinuma T, Igarashi A, Takigawa M, Nakanishi T, Takehara KJ. Role and interaction of connective tissue growth factor with transforming growth factor-beta in persistent fibrosis: a mouse fibrosis model. *J. Cell. Physiol*. 181:153-159. 1999.

152) Bartholin L, Wessner LL, Chirgwin JM, Guise TA. The human Cyr61 gene is a transcriptional target of transforming growth factor beta in cancer cells. *Cancer Lett.* doi:10.1016/j.canlet.2006.02.019. 2006.
153) Kato H, *et al.* Large-scale gene expression profiles, differentially represented in osteoarthritic synovium of the knee joint using cDNA microarray technology. Biomarkers. 12(4):384-402. 2007.
154) Aigner T, Zien A, Gehrsitz A, Gebhard PM, McKenna L. Anabolic and Catabolic Gene Expression Pattern Anaysis in Normal Versus Osteoarthritic Cartilage Using Complementary DNA-Array Technology. Arthritis and Rheumatism. 44(12):2777-2789. 2001.
155) Aigner T, Zien A, Hanish D, Zimmer, R. Gene Expression in Chondrocytes Assessed with Use of Microarrays. JBJS American. 85A(Suppl 2):117-123. 2003.
156) Galligan CL, Baig E, Bykerk V, Keystone V, Fish EN. Distinctive gene expression signatures in rheumatoid arthritis synovial tissue fibroblast cells: correlates with disease activity. Genes and Immunology. 8:480-491. 2007.
157) Eady JJ. Variation in gene expression profiles of peripheral blood mononuclear cells from healthy volunteers. Physiol Genomics. 22:402-411. 2005.
158) Clavet H, Hébert PC, Fergusson D, Doucette S, Trudel G. Joint Contractures Following Prolonged Stay in the Intensive Care Unit. CMAJ. 178(6):691-7. 2008.
159) Kellgren JH, JeffreyMR, Ball J. The epidemiology of chronic rheumatism. Atlas of standard radiographs of arthritis. Oxford, UK: Blackwell Scientific Publications, 1963:vii–11.
160) Wijbrandts CA, *et al.* Analysis of apoptosis in peripheral blood and synovial tissue very early after initiation of infliximab treatment in rheumatoid arthritis patients. Arthritis and Rheumatism. 58(11):3330-3339. 2008.
161) Hinman, *et al*. Is There an Alternative to the Full-Leg Radiograph for Determining Knee Joint Alignment in Osteoarthritis? Arthritis & Rheumatism. 55(2):306–313. 2006.
162) Kraus, *et al*. A comparative assessment of alignment angle of the knee by radiographic and physical examination methods. Arthritis & Rheumatism. 52(6):1730–1735. 2005.

Contribution of Collaborators

Thesis Supervisors

Dr. Guy Trudel and Dr. Odette Laneuville: guided project development, gave advice and provided teaching for experimental methods, provided regular direction to research and contributed intellectual content to thesis document.

Thesis Advisory Committee Members

Dr. Alain Stintzi, Dr. Zhara Montazeri, Dr. Julian Little: guided project development, gave advice and provided teaching for experimental methods, provided regular direction to research and contributed intellectual content to thesis document.

Contributing Partners

Dr. Hans Uhthoff: guided project development, gave advice and provided teaching for experimental methods, provided regular direction to research and contributed intellectual content to thesis document.

Mrs. Louise Pelletier and the University of Ottawa Pathology Department: provided guidance towards immunohistochemistry methods. Performed antigen retrieval, and certain parts of slide processing.

Mrs. Elizabeth Coletta: assisted with statistical analysis

Mrs. Ying Nie Ping: directed processing of samples destined for paraffin blocks. Assisted with histology and IHC methodology. Assisted with materials purchasing.

Dr. Mathew Quon: provided radiographic grading for subjects knee X-rays.

Dr. Natalie Buminov: provided guidance for many project methods including RNA extraction, PCR, lab reagents, and RNA purity evaluation.

Génome Québec: performed microarray hybridization after receiving isolated total RNA.

Orthopedic Research Department

Mrs. Sarah Plamondon: obtained consent from and recruited subjects for project. Measure knee ROM prior to TKA.

Mrs. Anna Fazekas: helped coordinate lab team and assisting members of orthopedic research department. Helped with subject recruitment planning.

Orthopedic Surgeons

Dr. Dervin, Dr. Kim, Dr. Feibel, Dr. Thurston, Dr. Beaulé: collected knee capsule tissue samples from subjects during TKA.

Curriculum Vitae

EDUCATION

2007 –2012	University of Ottawa Physical Medicine and Rehabilitation – Residency Program Fellow of the Royal College of Physicians of Canada (FRCPC)
2010 - Present	University of Ottawa Masters of Biochemistry (MSc) Candidate
2003 – 2007	University of Toronto Doctor of Medicine (MD)
1999-2003	McMaster University Honours Bachelor of Science (HBSc) Biochemistry with Molecular Biology Specialization and Honours Thesis Minor in Business

OTHER QUALIFICATIONS

Canadian Society of Clinical Neurophysiologists (CSCN) Diplomate (EMG)

LEADERSHIP, VOLUNTEER, AND EXTRACURRICULAR ACTIVITIES (RECENT)

July 2010 - June 2011	Chief Resident – University of Ottawa Physical Medicine and Rehabilitation
Webmaster – Department of Physical Medicine and Rehabilitation – University of Ottawa (Fall 2009-June 2011)	Maintained and updated the PM&R website for the University of Ottawa. http://www.ottawaphysiatry.com
International Health Volunteer - Friends of Honduran Children (Jan 2009, Jan 2007)	Provided primary medical care in rural areas of Honduras, Central America. Traveled with an inter professional group, the Peterborough Medical Brigade whose members included guides, doctors, nurses, a dentist, a pharmacist, and other volunteers.
French Language Training (Fall 2009, Winter 2007)	Provided by New Avenues Linguistics Services through the Ottawa Hospital. Completed levels 5 and 6 Advanced (7 levels in total).

Vice President Academic Inter Professional Healthcare Students' Association (IPHSA) (2006-07)	IPHSA: the first student organization at the University of Toronto to promote inter professional collaboration and to foster mutual understanding and respect among healthcare students. IPHSA is the U of T chapter of the National Health Sciences Student's Association (NaHSSA), the world's only national inter professional body governed by healthcare students. Members include students from Medicine, Pharmacy, Dentistry, Nursing, OT, PT, SLP, Medical radiation sciences, Social work, and Chiropractors. My initiatives in 2006-7 included: helping create an inter professional scholarship elective for junior healthcare students, overseeing the IPHSA essay competition, creating a case-based collaborative inter professional education (IPE) workshop, promoting current inter professional electives at U of T, expanding existing student IPE workshops, organizing student presentations describing the various disciplines, and assisting with other IPHSA initiatives.
President IPHSA (2005-06)	Officially founded IPHSA September 2005 as President. Obtained club status from the U of T Student Administrative Council and Student Affairs. Attended the NaHSSA conference in Vancouver as an IPHSA representative. Took responsibility for acquiring funds from professional associations and private entities for future NaHSSA sustainability. Personally involved in the organization and implementation of a number of inter professional initiatives in Toronto including student academic projects and presentations, IPHSA essay scholarship, IP athletics tournament, and social events. Attended and assisted in the planning of the 2006 NaHSSA Ontario Chapter conference.
Inter Professional Education (IPE) Representative, Faculty of Medicine (2004-05)	Elected position on class council. Worked with faculty members, the Medical Society and Student Council. Major initiatives included creating the Inter Professional Education student group as well as planning the inter professional showcase (students set up booths describing their professions in a hotel conference room) and social events during Pain Week (one week curriculum at U of T focusing on a multi-disciplinary approach to pain management).

PROFESSIONAL/WORK EXPERIENCE

Teacher / Instructor Kaplan (Jan–Mar 2005, Jun–Aug 2004)	Responsible for teaching the organic chemistry and biology sections to students preparing for the MCAT.
Research Assistant, McMaster University (Summer of 2002 and 2003)	Employed in a lab working on biochemical research at Hamilton Health Sciences Center under Dr. David Andrews. Responsibilities included planning/designing of experiments and interpretation of results.

HONOURS AND AWARDS

Physicians' Services Incorporated Foundation (2012)	Resident Research Prize for Excellence in Research Papers in the province of Ontario (1 of the top 5 resident research projects in the province)
University of Ottawa International Scholarship for New Faculty (2012-13)	Awarded to a resident graduate, nominated by the Division Chair, to travel abroad and develop skills to create innovative programs of excellence and enhance the educational and health care mandate at the University of Ottawa upon his or her return. Given for combined research and clinical Fellowship in Leeds, UK, Sept 2012-13.
Canadian Association of Physical Medicine & Rehabilitation – Resident Research Award: Best Project of the Year (2012)	Presented at the 60th CAPM&R Annual Scientific Meeting
University of Ottawa Division of Physiatry Resident Research Award - Best Presentation (2012)	Presented at the annual University of Ottawa Physiatry Day.
University of Ottawa Division of Physiatry Resident Research Award - Best Presentation (2011)	Presented at the annual University of Ottawa Physiatry Day.

University of Ottawa Division of Physiatry Resident Research Award - Best Presentation (2010)	Presented at the annual University of Ottawa Physiatry Day.
Inter Professional Education Leadership Award (2007)	Presented by the Office of Student Affairs, Faculty of Medicine, University of Toronto
Juanita Thompson Memorial Award (2007)	U of T Elective Award given to students to defray travel and maintenance expenses incurred during family practice electives. Received for travel to Honduras.
University (Senate) Scholarship at McMaster University	Made available by authorization of the Board of Governors of the University in recognition of outstanding achievement.
Dean's Honour List at McMaster University	Over entire undergraduate career.
Membership in the Golden Key Academic Honour Society	Membership is by invitation only to those students in the top 15% of their faculty in undergraduate years 2, 3, and 4.

RESEARCH

Oral Presentation: Campbell TM, Laneuville O, Uhthoff HK, Trudel G. Gene Expression in Patients with Severe Knee Osteoarthritis: Comparing Those With to Those Without Contracture. Canadian Physical Medicine and Rehabilitation annual Conference. June 2012.

Poster Presentation: Campbell TM, Laneuville O, Uhthoff HK, Trudel G. Protein Production in Patients with Severe Knee Osteoarthritis: Comparing Those With to Those Without Contracture. Canadian Physical Medicine and Rehabilitation annual Conference. June 2012.

Poster Presentation: Campbell TM, Laneuville O, Uhthoff HK, Trudel G. Histology of the Human Knee Capsule in End-stage Osteoarthritis With and Without Contracture. Canadian Physical Medicine and Rehabilitation annual Conference. June 2011.

Oral Presentation: Campbell TM, Laneuville O, Uhthoff HK, Quon M, Trudel G. Patients With Severe Osteoarthritis: Comparing Those With and Without Knee Flexion Contractures. Laurentian Conference of Rheumatology. May 2011.

Poster Presentation: Campbell TM, Laneuville O, Uhthoff HK, Quon M, Trudel G. Patients with Advanced Osteoarthritis of the Knee With and Without Flexion Contracture: Demographics and Associated Factors. Canadian Physical Medicine and Rehabilitation annual Conference. May 2010.

Undergraduate Thesis Project: Determining the Nature of the Loss of Viability in Sss1P Mutants. 2003. Supervisor: Dr. David Andrews

Acknowledged for experimental contribution in: Falcone D, Henderson MP, Nieuwland H, Coughlan CM, Brodsky JL, Andrews DW. Stability and Function of the Sec61 Translocation Complex Depends on the Sss1p Tail-Anchor Sequence. Biochemical Journal. Immediate publication March 1, 2011.

INTERESTS

Running
Weight Lifting
Hockey
Music
Computer Programs/Games